Soil nutrient variation along a shallow catena in Paracou, French Guiana

Leandro van Langenhove, Lore Verryckt, Clement Stahl, Elodie A Courtois, Ifigenia Urbina, Oriol Grau, Dolores Asensio, Guille Peguero, Olga Margalef, Vincent Freycon, et al.

Soil Research
2021, Volume 59 Issue 2 Pages 130-145
https://doi.org/10.1071/SR20023
https://archimer.ifremer.fr/doc/00656/76818/

Soil nutrient variation along a shallow catena in Paracou, French Guiana

Van Langenhove Leandro [1, *] , Verryckt Lore T. [1], Stahl Clement [2], Courtois Elodie A. [3], Urbina Ifigenia [4, 5], Grau Oriol [4, 5, 6], Asensio Dolores [4, 5], Peguero Guille [1, 4, 5], Margalef Olga [4, 5], Freycon Vincent [7, 8], Peñuelas Josep [4, 5], Janssens Ivan A. [1]

[1] Centre of Excellence GCE (Global Change Ecology), Department of Biology, University of Antwerp, Wilrijk, Belgium.
[2] INRA, UMR Ecology of Guiana Forests (Ecofog), AgroParisTech, Cirad, CNRS, Université de Guyane, Université des Antilles, 97387 Kourou, France.
[3] Laboratoire Ecologie, Évolution, Interactions des Systèmes amazoniens (LEEISA), Université de Guyane, CNRS, IFREMER, 97300 Cayenne, French Guiana.
[4] CSIC, Global Ecology Unit CREAF-CSIC-UAB, 08193 Bellaterra, Catalonia, Spain.
[5] CREAF, Cerdanyola del Vallès, 08193 Catalonia, Spain
[6] Cirad, UMR EcoFoG (AgroParisTech, CNRS, INRA, Université de Guyane, Université des Antilles), Campus Agronomique, 97310, Kourou, French Guiana.
[7] CIRAD, UPR Forêts et Societes, F-34398 Montpellier, France
[8] Forêts et Sociétés, Université de Montpellier, CIRAD, Montpellier, France.

* Corresponding author : Leandro Van Langenhove,
email address : leandro.vanlangenhove@uantwerpen.be

Abstract :

Tropical forests are generally considered to stand upon nutrient-poor soils, but soil nutrient concentrations and availabilities can vary greatly at local scale due to topographic effects on erosion and water drainage. In this study we physically and chemically characterised the soils of 12 study plots situated along a catena with a shallow slope in a tropical rainforest in French Guiana both during the wet and the dry season to evaluate seasonal differences. Soils along the catena were all Acrisols, but differed strongly in their water drainage flux. Over time, this differential drainage has led to differences in soil texture and mineral composition, affecting the adsorption of various nutrients, most importantly phosphorus. The more clayey soils situated on the slope of the catena had higher total concentrations of carbon, nitrogen, phosphorus and several micronutrients, while extractable nutrient concentrations were highest in the sandiest soils situated at the bottom of the catena. We found that carbon, nitrogen and extractable nutrients all varied seasonally, especially in the surface soil layer. These results are interesting because they show that, even at the local scale, small differences in topography can lead to large heterogeneity in nutrient concentrations, which can have large impacts on plant and microbial community organisation at the landscape level.

Keywords : French Guiana, lowland tropical forest, Paracou, phosphorus, topography, water drainage

Introduction

Tropical forests display notable heterogeneity in soil nutrient contents (Cuevas and Medina, 1986; Vitousek and Sanford, 1986; Laurance *et al.* 1999; Porder *et al.* 2005; Nardoto *et al.* 2008; Chadwick and Asner 2016), and nutrient constraints on ecosystem processes vary from local to regional scales in humid tropical lowland forests (Kaspari *et al.* 2008; Townsend *et al.* 2011; Wright *et al.* 2011; Alvarez-Clare *et al.* 2013). This variation is a product of unique and diverse combinations in the factors that regulate terrestrial ecosystem processes and soil development, i.e. parent material, time, climate, topography and biota (Jenny, 1941; Amundson and Jenny, 1997; Townsend *et al.* 2008). The heterogeneity of soil nutrients across diverse tropical landscapes presents challenges to understand and predict their ecosystem functioning (Randerson *et al.* 2009; Cleveland *et al.* 2011; Townsend *et al.* 2011). Identifying the drivers and

effects of this variation is essential as tropical forests play an important role in a range of global environmental change scenarios (Nemani *et al.* 2003; Clark 2004; Bonan, 2008) and in biogeochemical cycling (McGroddy and Silver, 2011).

Topography is one of the factors that contribute to landscape-scale variation in tropical nutrient distribution and, together with biota, likely has the greatest impact on local differences in soil development as time, climate and parent material are often relatively constant at the landscape scale. The impact of topography on soil formation is two-fold. On short timescales, high rainfall can cause hydrologic transport, redistributing nutrients and carbon (C) downslope and along flow paths (McSwiney *et al.* 2001; Chaves *et al.* 2009). On longer timescales, nutrient distribution is regulated through weathering, erosion and sediment transportation, all affecting soil development and residence times (Jenny, 1941; Walker and Syers, 1976; Tiessen *et al.* 1994; Birkeland, 1999). One of the major drivers of physical soil erosion and sediment transportation is slope steepness (Heimsath *et al.* 1997; Roering *et al.* 1999), which can play a major role in determining spatial patterns of nutrient availability across steeply dissected terrain (Porder *et al.* 2005; Weintraub *et al.* 2015). However, in low gradient landscapes with gentle slopes and continuous forest cover the rates of physical erosion and transportation are slower (Renard *et al.* 1997; Labrière *et al.* 2015), leading to increased importance of chemical weathering through the slow passage of water (Labrière *et al.* 2015). One example of low gradient landscapes with continuous forest cover is found in French Guiana, where landscapes are typically made up of a multitude of small hills and valleys, creating an undulating topography in which local hilltops descend towards stream beds over slopes with low inclinations (Boulet *et al.* 1979; Fritsch *et al.* 1986; Epron *et al.* 2006).

In French Guiana, the local hydrological regime has had a large influence on soil development, resulting in the formation of hydromorphic soils from ferralitic ones at the lower parts of the hills (Sabatier *et al.* 1997). Currently, nutrient poor Acrisols are found on the low elevation plateaus (Epron *et al.* 2006). They are dominated by low activity clays like kaolinite and gibbsite, but sesquioxide content is comparable to that of Ferralsols (Driessen *et al.* 2001). These sesquioxides are able to strongly sorb soil organic matter (SOM) and a variety of plant nutrients including phosphorus (P), greatly impacting its availability to the environment (Bortoluzzi *et al.* 2015). Over time, the passage of water has caused selective removal of the smallest particles, namely clay and associated secondary minerals, primarily on the lowest parts of the hillslopes (Chauvel *et al.* 1987; Dubroeucq and Volkoff 1998, Do Nascimiento *et al.* 2004; Epron *et al.* 2006). This means these soils are richer in quartz and poorer in clay content than their plateau counterparts, leading to differences in how nutrients are retained or leached out of the soil (Quesada *et al.* 2011). These differences can have profound effects on the standing biomass, and slight changes in soil properties of similar soils on a landscape scale had significant impacts on tree growth rate and mortality (Soong *et al.* 2020).

The tropical forests of French Guiana are affected by seasonally driven changes in precipitation and have a distinct wet and dry season. This is expected to influence pH, exchangeable cations (Sollins, 1998), and nutrient availability (Lodge *et al.* 1994; Campo *et al.* 1998; Chacón *et al.* 2008; Yamashita *et al.* 2010), notably as a pulse of nutrients at the onset of the wet season (e. g. Singh *et al.* 1989; Yavitt and Wright, 1996; McGrath *et al.* 2000; Yamashita *et al.* 2010). Several mechanisms could contribute to this seasonal variation in nutrient availability. For example, litterfall peaks at the onset of the dry season and accumulates until rainfall begins (Wieder and Wright, 1995; Chave *et al.* 2010;

Wagner *et al.* 2013), so nutrient mineralization from decomposing litter increases in the wet season. Phosphorus and other nutrients can be released from the soil microbial biomass by cell lysis when rapid rewetting follows an extended dry period (Sparling *et al.* 1985; Turner and Haygarth, 2001). Soil drying can also change soil physical and chemical properties, such as diffusion and oxygen availability, influencing nutrient concentrations (Birch, 1960; Bartlett and James, 1980; Tack *et al.* 2006). The effect of soil drying on nutrient concentrations, however, appears to vary among soils and nutrients (Turner et al. 2009). Seasonal variation in precipitation alters microbial communities, which can have an impact on the soil nutrient concentrations and affect the availability of these nutrients for plant growth (Smith *et al.* 2015; Turner *et al.* 2015; Yokobe *et al.* 2018).

The first objective of this study was to assess variation in chemical composition and fertility, namely total and extractable concentrations of various nutrients, along a low incline topographic gradient situated in Paracou, French Guiana. The second objective was to assess seasonal changes in chemical fertility on the same topographic gradient. For these purposes, we measured soil physical, mineralogical, and chemical properties on three distinct landscape units (top, slope and bottom) situated along a catena with a gentle slope (Fig. 1). We measured these variables once during the wet and once during the dry season in 2015.

We hypothesize that chemical fertility of the soil varies across the different landscape units due to differences in, e.g., mineralogy, particle size distribution, and hydrology, which affect soil nutrient adsorption capacities and availabilities in the soil. We also hypothesize that concentrations of extractable nutrients differ seasonally, as they can be affected by seasonal changes in, e.g., rainfall and humidity, decomposition of organic matter or associated microbial activity.

Materials and Methods

Study site

The study was conducted at the Paracou research station in French Guiana (Fig. 1 A and B). The station, 15 km inland from the coast (5°15'N, 52°55'W), covers 125 ha of primary lowland tropical forest. The site has between 150 and 200 tree species ha^{-1} and a stand density of on average 450 trees ha^{-1} (DBH> 10 cm). The most represented plant families occurring at the site are the Lecythidaceae, Fabaceae, Sapotaceae and Chrysobalanaceae, but detailed descriptions of the floristic composition can be found in Gourlet-Fleury et al. (2004). Average annual rainfall and air temperature for the period 2004-2014 at the study site was 3102 ± 70 mm and 25.7 ± 0.1 °C, respectively, while average wind speed is between 2 and 5 km h^{-1} predominantly from a northeast direction (Aguilos *et al.* 2019). The French Guianese climate is characterized by a wet and a dry season due to the north/south movement of the intertropical convergence zone. The wet season extends from December to July and peaks in May when monthly rainfall typically exceeds 600 mm. The dry season, characterized by less than 100 mm monthly rainfall, is from August to November (Aguilos *et al.* 2019). The wet season sampling was carried out between May 29th and June 10th 2015, just after the period with the heaviest rainfall occurring in May (Fig. S1). The dry season sampling was carried out between October 5th and October 21st 2015, in the third month of the dry season (Fig. S1).

Paracou is located on the smoothest landscape units found on the schist of the Bonidoro series (Gourlet-Fleury *et al.* 2004), rich in muscovite and containing veins of pegmatite of variable size (Sabatier *et al.* 1997). The landscape is a tabular system incised by streams and altitudes range from about 15 to 50 m above sea level (Fig. 1 C). Topography is undulating with maximum slopes of approximately 30°. On average, the elevational differences between hill summits

and valleys are 40 m over horizontal distances of 200 to 400 m. At the Paracou research site, soils are characterized as nutrient-poor Acrisols (FAO, 1998) in which total and available P content is low (Grau *et al.* 2017). Over time, local differences in weathering and hydrology have led to spatial variability in soil type across the French Guiana soils, but all are ordered on the landscape scale. Detailed studies of elementary catchments in French Guiana (Boulet, 1983; Fritsch *et al.* 1986) have enabled the identification of four stages of soil evolution developed on the ferralitic bedrock cover (Boulet *et al.* 1993). At Paracou, the soils have reached the fourth stage of evolution, meaning that soil transformation has been ongoing under hydromorphic conditions, causing a redistribution of iron downhill. We refer to Sabatier *et al.* (1997) for more details on soil evolution in Paracou.

Experimental design

We identified three distinct landscape units upon a toposequence that showed an altitudinal decline of about 20 m over about 200 m distance. These landscape units were (1) bottom, i.e. just above the creek running through the valley, (2) slope, i.e. the intermediate section of the elevation, and (3) top, i.e., where the slope evens out and becomes the hilltop. On each landscape unit we established four plots of 50 x 50 m each (see Courtois *et al.* 2018 and Fig. 1 D and E) and sampled soils within a visually homogenous 20 x 20 m area within the larger 50 x 50 m plot (Fig. 1 F). Distances between the plots were 10 – 100 m. In two of our top plots we observed clear depressions in the soil, so-called Djougoung-Pétés, that indicate ancient tree falls and, because of the presence of a clay-rich drainage barrier near the surface, often show standing water up to 72 h after rainfall (Blancaneaux, 1973). We did not sample within 2 m of such a depression in the soil.

Soil sampling

Sampling of the various soil samples was done manually using different augers during the 2015 wet season (May 2015). Once per plot, we used an Edelman auger (6 cm diameter) to sample to a 1.2 m depth (0.1 m, 0.2 m and every 0.2 m below) for visual soil classification. At five locations in each plot, we used an auger with a 15 cm long cylindrical head (8 cm diameter) to sample bulk density to a depth of 30 cm. Lastly, we used a gouge auger (5 cm diameter) at five locations inside each plot to extract soil samples for chemical analysis to a depth of 30 cm (Fig. 1 F). This last sampling was carried out twice (once in the wet and once in the dry season) to look at seasonal changes in the chemical soil properties. Samples used for soil particle size distribution analysis, X-ray diffraction (XRD) and chemical analyses were sieved (2 mm) fresh. We chose to divide the soil into a 'surface' layer (0 – 15 cm) and a 'deeper' layer (15 – 30 cm) instead of sampling by genetic horizon because the upper horizon in Paracou varies between 0 - 15 and 0 - 20 cm depth while the next horizon often extends to 50 cm depth and beyond (Guitet *et al.* 2015). Additionally, this standardization would allow more accurate bulk density measurements and calculations of nutrient stocks by soil depth.

Soil physical properties

Visual soil classification was done on the single (per plot) 1.2 m soil core extracted with the Edelman auger. Soil moisture and texture (by touch), colour (Munsell code), as well as the presence of stones or coloured spots were examined and used to classify soils. The depth of the clay rich drainage barrier was subjectively localized by manual perception of clay content and silt dryness. The appearance of the 'dry to the touch' character at a depth of less than 1.2 m was used to discriminate soils exhibiting vertical drainage from soils exhibiting

193 superficial lateral drainage (adapted from Boulet *et al.* 1983; Sabatier *et al.*
194 1997).

195 Soil bulk density samples were sieved through a 2 mm sieve. Soil weight was then
196 determined after drying at 105°C during 24 h and divided by the corer volume to
197 obtain the bulk soil density. Volumetric water content (SWC_{Vol}) was calculated
198 by multiplying the gravimetric water content with the bulk soil density and
199 dividing by the water density, which we assumed was 1 g cm^{-3}. We used a neural
200 network prediction (Rosetta Lite version 1.1; Schaap *et al.* 2001) function based
201 on pedotransfer functions (PTF's) to estimate van Genuchten (1980) water
202 retention parameters. These parameters allowed us to build a water retention
203 curve for each plot and from this curve extract the SWC_{Vol} at which field capacity
204 (FC) was reached. We then expressed the measured SWC_{Vol} as a percentage of
205 FC. (SWC_{Per}) to allow direct soil moisture comparisons between soils. For a more
206 detailed description we refer to Schaap *et al.* (2001).

207 For both particle size distribution analysis and measurements of XRD aliquots of
208 the five previously sieved samples extracted using the gouge auger were mixed
209 together by hand per depth (0 – 15 cm 'surface' and 15 – 30 cm 'deeper') and
210 analysed as one composite sample per depth and per plot. Soil particle size
211 distribution was determined using the hydrometer method (Gee and Bauder,
212 1986) following soil organic matter oxidation with H_2O_2. Soil particles were
213 dispersed with sodium hexametaphosphate and the amounts of sand, silt and
214 clay were determined using a hydrometer. For XRD analysis we used an X'Pert
215 PRO MPD powder diffractometer (Malvern Panalytical, UK) in a Bragg-Brentano
216 $\theta/2\theta$ reflection configuration with $K\alpha_1$ radiation (λ=1.5406 Å) , selected by means
217 of a primary Ge (111) Johansson type primary monochromator, and X'Celerator
218 1D silicon strip detector (active length 2.122 °2θ), at the X-Ray Diffraction Unit
219 of the Scientific and Technological Centers of the Universitat de Barcelona. Dried

and ground soil samples were mounted in standard cylindrical sample holders, of Ø 16 mm and *h* 2.5 mm, to obtain powder XRD diagrams from 3 to 80 °2θ, step size 0.017 °2θ and measuring time of 50 seconds per step (30 minutes of total measuring time), with constant illuminated area of 10 x 12 mm and sample rotation at 2 seconds per revolution. The qualitative mineral phase analysis was performed with the aid of the Powder Diffraction File Data base PDF-4+ 2020 (ICDD, 2016) and through the X'Pert HighScore Plus software, version 4.7, 2017 (Degen *et al.* 2014). See table S1 in the supplementary information for the reference numbers of each evaluated mineral.

Chemical analyses

Aliquots from the previously sieved soil samples gathered with the gouge auger were divided into two parts. The first part was oven dried at 70 °C during two days to determine gravimetric water content by measuring weight loss. Dried soil was then ground in a ball mill (Retsch, Germany) and used to determine the concentrations of C and N through dry combustion with an elemental analyser (Flash 2000, Thermo Fisher Scientific, Germany) and also to determine the concentrations of P, K, S, Ca, Mg, Fe, Mo, Cu, Mn, Na, Zn, Ni, V, Cr, As, Sr and Cd through acid digestion in a ultraWAVE digestor (Milestone, Italy) followed by ICP-MS (7500 ce model, Agilent, USA). The second part of the sieved soil was used for the measurement of pH and the extraction of inorganic N and P. The pH was measured by adding 1M KCl to the soil in a 1:2.5 w:v ratio, shaking for 1 h and measuring with a pH meter (HI 2210-01, Hanna Instruments, USA). The same soil solution was passed through a 42 µm filter and the filtrate's concentration of NH_4^+ and NO_3^- was determined colorimetrically (SAN++ continuous flow analyser, Skalar Inc, The Netherlands). Inorganic P was determined in two ways, the Bray-P acid fluoride extraction (Bray and Kurtz 1945) and the Olsen-P bicarbonate extraction (Olsen *et al.* 1954). Phosphorus concentrations in both

extracts were measured with an iCAP 6300 Duo ICP optical emission spectrometer (Thermo Fisher Scientific, Germany).

Data analysis

We employed a multivariate approach to examine whether total element profiles differed along the toposequence. The concentrations of sixteen elements measured in the soil at the three landscape positions were used for this multivariate analysis: C, N, P, K, Mg, Fe, Mo, Cu, Mn, Zn, Ni, V, Cr, As, Sr and Pb. These metrics were used to create a distance matrix and conduct a principal component analysis (PCA) after which a PERMANOVA test assessed differences in integrated elemental concentrations with landscape position and season (Anderson 2017). If the PERMANOVA test indicated a significant effect a beta dispersion test was conducted to check centroid dispersion (Anderson *et al.* 2011). In addition, we analysed these sixteen elements and the concentrations of inorganic N and P individually to examine which ones differed by landscape position and season. Linear mixed-effects models (LMM) were employed, with topographic position (bottom, slope or top) and season (wet or dry) as fixed effects and plot as random effect. Prior to analysis, data were log transformed if needed, to match normality assumptions. Multiple comparisons within a factor were analysed using Tukey *post hoc* tests. We used Pearson correlations to examine the relationship between soil clay content and the concentrations of the various elements that significantly changed over one or multiple landscape units. When examining the association between inorganic P and total Fe concentrations using Pearson correlations we visually observed a trend break in the relationship. We confirmed that the slope of the regression before the trend break was significantly different from the slope of the regression after the trend break using a piecewise regression model. The validity of the models' assumptions (linearity, normality of residuals, no influential outliers,

274 homoscedasticity) were evaluated with standard functions of R, including
275 diagnostic plots. All analyses were performed in R 3.5 (R Core Team 2018) and
276 we used the packages dplyr (Wickham *et al.* 2018), ade4 (Dray and Dufour,
277 2007), vegan (Oksanen *et al.* 2019) and lmertest (Kuznetsova *et al.* 2017) for
278 calculations and ggplot2 (Wickham *et al.* 2016) for visualizations.

Results

Soil classification

Overall, sand particles (> 53 µm) dominated soil profiles across the site's topographical gradient (average 72 % by mass), while clay particles (< 2 µm) only accounted for 12 % of soil particles in the upper 15 cm, and 14 % in the deeper soil (15-30 cm). Slope soils were, however, significantly ($P < 0.05$) richer in clay than bottom or top soils at both depths (Table 1). The XRD analysis showed that soils were characterized by different proportions of four main minerals (Table 1) with quartz (SiO_2) being the dominant primary phase, inherited from the weathered bedrock. The other three phases were kaolinite (1:1 clay $Al_2Si_2O_5(OH)_4$), gibbsite (aluminium hydroxide, $Al(OH)_3$) and iron (hydr)oxides ($FeO(OH)$ and Fe_2O_3), all neoformed clay-sized minerals typical of highly weathered tropical soils. The XRD results also showed that slope and top soils had similar proportions of mineral phases while bottom soils were significantly different. Bottom soils contained more sand and consisted of 80 % quartz, 15 % kaolinite, 4 % gibbsite and a very low proportion of Fe (hydr)oxides (+- 1.5 %). In comparison, slope and top soils had lower proportions of quartz (60 – 70 %) and higher proportions of kaolinite (20 – 30 %) and Fe (hydr)oxides (+- 5%, Table 1).

Soils from the different plots within a single landscape unit (bottom, slope or top) exhibited heterogeneity in their drainage conditions, especially on the top. There, we found two plots showing slowed vertical drainage due to a reddish brown clayey horizon with a micro-aggregated structure followed by a red clayey weathered horizon at a depth of less than 1.2 m (ferralic acrisol). The two other plots, along with all slope plots, showed superficial lateral drainage because of a clay rich drainage barrier at a depth between 40 and 80 cm (haplic acrisol), that restricted the vertical drainage. On the valley bottom, soils were hydromorphic

and in two plots the water table occasionally reached the surface horizon (ferric acrisol). They were wet to the touch and exhibited red and yellow mottled saprolite at a depth of less than 1.2 m. The soil of the two other bottom plots was strongly hydromorphic, and the water table was present in the surface horizon (gleyic acrisol) as indicated by the light grey to white soil colour indicating reductomorphic properties. This soil was very wet to the touch and had the lowest clay content of all plots, both in the surface layer (0 – 15 cm, < 7 %) and deeper layer (15 – 30 cm, < 10 %).

The pH across all soil samples was acidic and ranged between 3.64 and 4.90. With the exception of top landscape unit surface soil, which was slightly more acidic than bottom soil, there were no topographical or seasonal differences in pH. The pH in the deeper soil layer was slightly higher than in the surface soil layer. Averaged over both soil depths, volumetric soil water content (SWC_{Vol}) decreased by 5.2 % (SE 1.5 %) during the dry season ($P < 0.001$), while it decreased by 3.1 % (SE 1.7 %) with depth ($P < 0.01$) when averaged over both seasons. Overall, within a given soil depth and season, the percentage of SWC_{Vol} relative to SWC_{Vol} at Field Capacity (SWC_{rel}) was equal in bottom and slope landscape units, while top SWC_{rel} was lower. In the surface soil layer during the wet season, both bottom and slope SWC_{Vol} were roughly equal to Field Capacity (~ 100 %), while in the deeper soil layer this was only 81.3 % and 65.5 %, respectively. Top plot SWC_{rel} consequently indicated drier soils that, even in the wet season, did not reach 70 % SWC_{rel} (Table 2 and 3).

Soil elemental concentrations and stocks

We found that the concentrations of soil C, N and P correlated well with clay content in both soil layers (Fig 2). Overall, this was also true for the metals Mo, Zn, Cu and Ni (Fig 3). The correlations of C, N, Mo, Cu and Ni with clay content were strongest in the deeper soil layer, while this was opposite for P and Zn.

The PCA and subsequent PERMANOVA test conducted on the combined total elemental concentrations from both soil depths revealed significant differences in element concentrations with depth ($F_{1,228} = 5.04$, $P < 0.05$). The beta dispersity test was negative, showing that this result was not confounded by centroid dispersion. Therefore, we analysed the two sampled soil layers separately and conducted a PCA analysis for each soil layer.

In both soil depths the PCA (Fig 4) and subsequent PERMANOVA test conducted on the total elemental concentrations (C, N, P, K, Mg, Fe, Mo, Cu, Mn, Zn, Ni, V, Cr, As, Sr and Pb) showed a significant effect of topographical position ($F_{2,113} = 4.0$, $P < 0.05$ and $F_{2,111} = 3.7$, $P < 0.05$ for surface and deeper layer, respectively), while no effect of season was observed at either depth. However, the beta dispersity test yielded a significant result for topographical group dispersion in both soil depths (surface layer: $p < 0.01$ and deeper layer: $p < 0.001$), indicating that there was significant dispersion from the centroid. Thus, we cannot be sure that the observed differences in elements as found by the PERMANOVA were indeed true topography-induced differences and not the result of differences in group dispersion. Topographical differences are discussed further in function of the PCA, but instead analysed with linear mixed effects models.

The principal component (PC) 1 of the surface soil elemental PCA, which explained 36.9 % of the variation, was mainly driven by the concentrations of the metals Fe, Cu, Ni, V, Cr and As (Table S4 and S5). In the deeper soil layer PC1 explained 35.1 % of the variation and was again mainly driven by the concentrations of the metals Fe, Cu, V, Cr and As, but, in contrast to the surface soil, here Ni did not participate in driving PC1 while Mn did. PC2, which explained 16.9 % of the variation in the surface soil and 18.9 % of the variation in the deeper soil layer, was mainly driven by the concentrations of C, the macro nutrients N and P, and Pb in both soil layers (Table S4 and S5).

Depth

When examined individually, concentrations of nine out of the sixteen studied elements differed between the surface and deeper soil. Carbon, N, P and Mg concentrations decreased with depth, while K, Fe, Ni, V and As concentrations increased with depth. Depth had no impact on the concentrations of Mo, Cu, Mn, Zn, Cr, Sr and Pb. This was true in the three sampled landscape units.

Topography

Within soil layers, the concentrations of three and eight of the sixteen elements differed among landscape positions in the surface and deeper soil, respectively. Surface soil P concentrations were highest on the slopes and significantly lower on bottom and top ($P < 0.01$ for all comparisons). Deeper-soil C, N and P concentrations were higher in the slope plots than in the top plots ($P < 0.05$ for all), while bottom concentrations were not significantly different from either slope or top concentrations, with the exception of total P which was different ($P< 0.001$) from slope total P and equal to top total P. Additionally, in both soil layers, measured concentrations of Fe and Mn were lowest at the bottom and significantly higher on the top and, in the case of Fe, on the slope landscape positions. For Mn, we found that slope concentrations were not different from either bottom or top concentrations, but rather were intermediate between the two (Table 2 and 3).

Exclusively in the deeper soil layer, we found that the concentrations of heavy metals Mo, Cu, Zn and Ni varied with changing topography. Lowest concentrations occurred in the bottom plots, and highest concentrations in the slope plots. Top plot Mo and Cu concentrations were intermediate between bottom and slope, while Zn and Ni concentrations were not different from concentrations in slope plots. Lastly, in surface soils, the difference in the

concentrations of Mo, Cu and Ni between bottom and slope plots was nearly significant ($P < 0.07$ in all cases, Table 3).

Seasonality

In the surface soil (Table 2), seasonality had an effect on the concentrations of C, N and Mg. Carbon and N concentrations were higher in the dry season than in the wet season ($P < 0.001$ for both), while the opposite was true for Mg, which was highest in the wet season ($P < 0.001$) and declined in bottom and slope landscape units during the dry season. There was no decline of Mg concentration in the top landscape during the dry season. With the exception of C and N, we observed no effect of seasonality on any of the measured nutrient concentrations in the deeper soil layer (Table 3). Similar as in the surface soil layer where the concentrations of both C and N were higher during the dry season ($P < 0.01$ for both).

Nutrient extractions

The concentrations of extractable N and P (as proxies for their availability) varied with depth, landscape position and season. The surface soil concentrations of ammonium (NH_4^+), nitrate (NO_3^-), Bray extractable P (P_{Bray}) and Olsen extractable P (P_{Olsen}) were all higher ($P < 0.001$ for all) than those in the deeper soil layer (Table 2 and 3). Surface and deeper soil NH_4^+ concentrations were highest ($P < 0.01$) in the slope plots and lowest in the bottom plots, while top concentrations did not significantly differ from either bottom or slope plots ($P= 0.12$ and $P = 0.07$, respectively). Concentrations of NO_3^- did not vary topographically in either soil layer. In surface and deeper soil, the P_{Bray} and P_{Olsen} concentrations were both low and similar to each other. Both concentrations were highest ($P < 0.001$ for both) on the bottom landscape position and decreased towards the slope and top, with slope and top concentrations not differing from each other. In the surface soil layer there was a large effect of seasonality and concentrations of

extractable N and P were all lower in the dry season ($P < 0.001$ for all). In the deeper soil layer seasonality only impacted the extractable N concentrations, lowering them significantly ($P < 0.001$), while the concentrations of extractable P remained unchanged. There was a strong negative correlation between P_{Bray} and total Fe in both soil layers, but only until Fe concentrations reached 20 g kg^{-1}. There occurred a trend break in the correlation around 20 g Fe kg^{-1} (piecewise regression, $P < 0.001$), above which higher Fe concentrations no longer correlated with a decline in P_{Bray} (Fig 5).

Discussion

Our results concur with previous studies suggesting that nutrient distribution can vary along local topographic gradients (Tiessen *et al.* 1994; Scatena and Lugo, 1995; Vitousek *et al.* 2003; Porder *et al.* 2005; Weintraub *et al.* 2015; Osborne *et al.* 2017), although in our study not all assessed nutrients differed along the topographic gradient.

Soil description

In soils that are vertically draining the water percolates downwards and leaches aluminium from the clay minerals (here predominantly kaolinite and gibbsite, see Table 1), while the sand, which here is quartz dominated, stays in place, resulting in a relative enrichment of sand (Lucas and Chauvel, 1992). In soils that are draining laterally this process is slower, resulting in less aluminium leaching and thus a relatively higher clay content than the vertically draining soils (Lucas and Chauvel, 1992). This explains the higher clay content found on our slope plots, where lateral drainage predominates, and where surface run-off further contributes to reduced vertical drainage. In contrast, the ferric and gleyic acrisols on the bottom landscape have undergone intense chemical weathering due to the influence of water, which is found, on average, at a depth of 18 cm (Ferry *et*

al. 2010). This resulted in leaching losses of Fe, Al and organic colloids, mainly preserving the more stable minerals such as quartz (Lucas *et al.* 1996). Comparing the calculated values of SWC_{Per} with the soil water potential profiles from Sabatier *et al.* (1997) confirms that our bottom landscape has a combination of ferric acrisol and gleyic acrisol soils.

Topographic differences in soil nutrients

At the catena scale, P, Fe and Mn varied topographically in both the surface (0-15 cm) and deeper (15-30 cm) soil layers, while C, N and the metals Mo, Cu, Zn and Ni varied topographically in the deeper soil layer only. The concentrations of total P in the soil were very low across all topographies, ranging between 22 and 254 mg kg^{-1}, which is a direct result of weathering since the Precambrian that has led to the depletion of P in the soils situated upon the Guiana Shield (Walker and Syers, 1976; Vitousek and Howarth, 1991; Hammond *et al.* 2005). Low concentrations of both total and extractable soil P are typically found in Amazonian primary tropical forests situated on old and highly weathered soils (Quesada et al; 2010), and as total P decreases the remaining P pool is gradually transformed into more recalcitrant, occluded forms (Walker, 1964; Smeck, 1973; Tiessen *et al.* 1984; Crews *et al.* 1995). Occlusion mainly occurs on incompletely weathered mineral surfaces, such as kaolinite, or on secondary minerals (Yang et al; 2013), such as the overly abundant metal (hydr)oxides (Sanchez, 1977). Both are linked to clay content, explaining why we found a strong correlation between soil P and the clay fraction (Fig 3).

The concentrations of Fe were much lower in the bottom landscape than on the slopes and tops, which is likely related to waterlogged conditions occurring more frequently on the bottom landscape position (Ferry *et al.* 2010). These can cause temporal anoxic conditions in the soil, contributing to the development of the gleyic acrisol we observed (Setter and Waters, 2003; Gross *et al.* 2018). Under

anoxic conditions, Fe(III), present in the Fe-(hydr)oxides in the mineral clay fraction, becomes the dominant terminal electron acceptor (Hall and Silver, 2015) and is reduced into Fe(II). Reduced Fe(II) is water soluble (Chacón *et al.* 2006) and more easily leached out of the soil. Over time, these leaching losses lead to lower Fe concentrations in the ferric and gleyic acrisols found at our bottom landscape than in the vertically and laterally draining slope and top soils (Tables 2 and 3).

As Fe(hydr)-oxides are washed away over time by water moving through the soil layer, the capacity of the soil to strongly bind P decreases. Combined with higher diffusion rates due to the proximity of the water table, this then increases the concentration of extractable P_i, provided there is sufficient accumulation of microbial biomass between flooding events and introduction of decomposable organic material (Chacón *et al.* 2005), from which P_i can be released. The increase in extractable P_i in bottom plots occurred together with the lowest activity of acid phosphatase in soil as compared to slope and top plots (Fig. S2). This is in agreement with the generally observed negative relationship between phosphatase activity and P_i (Sinsabaugh and Shah, 2012; but see Margalef *et al.* 2017) and suggests that drainage characteristics are important for determining plant and microbial activities in this ecosystem. Specifically in Paracou, Allié *et al.* (2015) reported similar ranges of extractable P_i, with highest concentrations occurring at the lowest part of the valley, just as found in the current study.

Though not a direct measure of Fe-(hydr)oxide presence, we can assume that higher concentrations of Fe in the soil are linked to higher concentrations of Fe-(hydr)oxides. The finding that both total Fe and iron oxide percentage were lowest on the bottom landscape positions reinforces this assumption (Table 1, 2 and 3). When more Fe-(hydr)oxides are present in the soil, more P can be occluded. This decreases extractable P_i in the soil solution. We observed a

492 negative and logarithmic correlation between the extractable P_i and Fe
493 concentrations (Fig 5), indicating that extractable P_i indeed decreases when
494 more Fe is present in the soil. However, we also observed that once the Fe
495 concentration reached 20 g kg^{-1} or more there was no further decline of
496 extractable P_i (Fig 5). This is likely because P solubility (sorption and desorption)
497 is in equilibrium and even at high metal(hydr)-oxide concentrations a minimum
498 of P_i remains in the soil solution (Pierzynski and McDowell, 2005). As extractable
499 P_i is removed from the soil solution by plant, mycorrhizal or microbial uptake, P
500 exchange kinetics ensure that P_i in the soil solution is replenished by P from the
501 soil solid phase (Helfenstein *et al.* 2018).

502 It is noteworthy that, despite the negative correlation between soil extractable
503 P_i and soil Fe content (Fig 5), we found no significant correlation between total
504 P and soil Fe content. This is likely because not only Fe(hydr)-oxides are occluding
505 P, but also Al(hydr)-oxides and Mn(hydr)-oxides, which are also part of the clay
506 size fraction of the soil (Barrón and Torrent, 2013).

507 Although we were unable to quantify the Al concentration in our soils, we found
508 that the gibbsite content was relatively high in the bottom and slope topographic
509 positions. As gibbsite is one of the mineral forms of Al hydroxide we can assume
510 that Al hydroxides played a role in occluding P, obscuring any linear relationship
511 between soil P and Fe. Similarly to Fe(II), reduced Mn(II) is water-soluble and can
512 be leached out (Barrón and Torrent, 2013), likely explaining why we found lower
513 concentrations in the bottom topography than on the slope or top. However, the
514 concentration of Mn was much lower than the Fe concentration (between 150
515 and 1500 times lower, Tables 2 and 3), thus making it unlikely that Mn(hydr)-
516 oxides played a large role in P occlusion in our soils. Lastly, a fraction of the total
517 P is also associated with soil organic matter, which can even interfere with P
518 adsorption unto metal oxides under specific conditions (Sibanda and Young,

519 1986; Antelo *et al.* 2007; Yan *et al.* 2016; Fink *et al.* 2016). Together, this means
520 that total P concentration is unlikely to be directly correlated with any one
521 variable, with the exception of clay content as was found here (Fig 2 e and f).
522 This is because most, if not all, metal(hydr)-oxides are found within the clay
523 particle size fraction of the soil and, additionally, clay minerals can adsorb soil
524 organic matter (SOM) containing P (Lagaly *et al.* 1984).

525 As is typical for forest soils (e g. Chauvel *et al.* 1987; Jobbágy and Jackson, 2000),
526 the surface soil layer had higher concentrations of soil organic C (SOC) and total
527 N than the deeper soil layer. We observed no topographical variation in SOC or
528 in total N in the surface soil layer, but did find significant correlations with clay
529 content in both soil layers (Fig 2). The lack of topographical variation was
530 different from results reported by topographical studies conducted nearby
531 Manaus, Brazil (Luizão *et al.* 2004) and, for C only, at the same Paracou study site
532 in French Guiana where a modest topographical effect was found (Epron *et al.*
533 2006). Both studies linked topographical differences in SOC to the higher clay
534 mineral content found on their upslope topographies, which favours aggregate
535 formation resulting in an effective retention of SOM especially under acidic
536 conditions (Sposito, 1996; Hernández-Soriano, 2012). However, the range of
537 topographical variation in clay content found previously in Manaus (Luizão *et al.*
538 2004) and Paracou (Epron *et al.* 2006) was much larger than the range identified
539 in the plots here, namely 5 – 65 % and 6 – 36 %, respectively, versus 6- 23 %. It
540 is possible that the smaller topographical variation in clay content obscured a
541 significant topographical effect on SOC content, in spite of a significant positive
542 correlation between the two (Fig 2).

543 The concentrations of the metals Mo, Zn, Cu and Ni in the deeper soil layer all
544 varied with topography, and highest concentrations occurred on the slopes,
545 while lowest were consistently found in the bottom landscape plots. With the

546 exception of Zn, the concentrations of these metals correlated positively with
547 clay content in the deeper soil layer (Fig 4 b, f and h). The clay fraction of the soil
548 can hold the highest concentration of a variety of metals, up to 375 times more
549 than sand (Harter and Naidu, 1995; Quenea *et al.* 2009), a characteristic that
550 makes the clay content of the soil one of the main determinants of retention of
551 a variety of metal ions (González-Costa *et al.* 2017). That deeper soil layer Zn
552 concentrations did not correlate with clay content was likely related to the clay
553 minerals present in our soils. According to González-Costa *et al.* (2017), chlorite
554 is the most important clay mineral involved in the adsorption of Zn, followed by
555 gibbsite, vermiculite and finally kaolinite. Although soils developed on the
556 Bonidoro formation, such as the soils in this study, can contain modest amounts
557 of chlorite (Kroonenberg *et al.* 2016), we found none in this study. Soil
558 phosphatase activity was also significantly higher on the slopes, in both soil
559 layers (Fig S2), suggesting a higher dominance of extracellular enzymes stabilized
560 by sorption to clay and silt or to organic matter (Sarkar *et al.* 1989; Lee *et al.*
561 2007).

562 The modest amount of gibbsite and the high amount of kaolinite we identified
563 could then explain why there was no correlation between Zn and clay content.
564 In contrast with the deeper soil layer, there was no topographical variation in
565 Mo, Zn, Cu and Ni concentration in the surface soil layer. It is likely that, due to
566 its capacity to strongly sorb metals (Gustafsson *et al.* 2003) while decomposing,
567 its higher concentration and its more or less even distribution along the
568 topographic gradient in the surface soil layer, the SOM content may have been
569 obscuring potential topographic differences in Mo, Zn, Cu and Ni concentrations
570 related to differing particle size distributions.

571 Seasonal differences in soil nutrients

572 We observed seasonal variation in the concentrations of C, N, Mg and the
573 extractable N_i and P_i. Typically, at the onset of the dry season, there is an increase
574 in leaf abscission and flushing of new leaves, resulting in increased litterfall
575 across tropical south America (Myneni *et al.* 2007; Chave *et al.* 2010) and,
576 specifically, in Paracou (Wagner *et al.* 2013). This leads to accumulation of
577 organic matter in the soil and thus higher concentrations of C and N during the
578 dry season. At the same time, microbial biomass (Singh *et al.* 1991; Luizao *et al.*
579 1992; Srivastava, 1992; Henrot and Robertson, 1994; Cleveland *et al.* 2004) and
580 activity (Cleveland *et al.* 2004; Turner *et al.* 2013) decrease, reducing litter
581 decomposition. In our study, lower microbial and plant activity during the dry
582 season were reflected by the lower acid phosphatase activity during this period
583 (Fig S2). This then leads to lower concentrations of extractable N and P as
584 compared to the wet season. The return of the wet season rains can initiate
585 synchronous decomposition of litter accumulated over the dry season (McGrath
586 *et al.* 2000), resulting in pulsed nutrient mineralization and increases in
587 extractable N and P (Lodge *et al.* 1994). The observed decrease in nitrate
588 concentrations contrasts to results reported from Costa Rica, where nitrate
589 concentrations were highest during the dry season (Koehler *et al.* 2009; Turner
590 *et al.* 2013). They attributed this increase to reduced nitrate leaching and
591 denitrification processes in the absence of rainfall, both processes that were not
592 measured in this study.

593 In contrast to other cations like K, Ca and NH_4^+ is Mg comparatively mobile in
594 soils (Gransee and Führs 2012). In acidic soils with a clay fraction dominated by
595 low activity clays the majority of Mg is commonly found in the soil solution,
596 making it susceptible to leaching (Mesić et al. 2007). During the wet season,

when soils contain more water than during the dry season, this leads to higher soil Mg concentrations.

Conclusion

The current distribution of the different soil types along the catena is largely due to the water movement through these soils. This has modified the particle size distribution in these soils, resulting in more sandy soils on the bottom topography, while the soils containing the most clay remain on the slopes. Water drainage also caused the unequal distribution of Fe along the catena. The more frequent occurrence of anoxic conditions in the bottom soil also affected the metal (hydr)oxides' oxidation status, which in turn reduced their P occlusion capacity. Because of this reduced ability to occlude P, extractable P_i was higher in the bottom landscape resulting in higher soil fertility which is important for tree growth there. Lower Fe concentrations also correlated with higher concentrations of P_i. When less Fe-(hydr)oxides are present in the soil, the capacity of the soil to occlude and bind P is lowered, resulting in higher concentrations of unbound P_i in the soil solution.

Overall, our results suggest that topography plays an important role in the determination of total and extractable nutrients in this tropical forest through differences in the distribution and redox status of clay particles along the catena.

Finally, seasonal differences were observed in the SOC, SON and the extractable N and P. This is related to the increased input of organic matter occurring during the dry season that is not immediately decomposed because of microbial water stress. This then results in increased SOC and SON contents during the dry season. Decreased decomposition leads to decreased amounts of extractable P_i and Ni in the soil solution, explaining why we found lower concentrations during the dry season than in the wet season, when decomposition rates go up.

Conflicts of interest

The authors declare no conflicts of interest.

Acknowledgements

This research was supported by the European Research Council Synergy grant ERC-2013-SyG. 610028-IMBALANCE-P. We thank the staff of the Paracou station, managed by UMR Ecofog (CIRAD, INRA; Kourou). The research station received support from “Investissement d’Avenir” grants managed by Agence Nationale de la Recherche (CEBA: ANR-10-LABX-25-01, ANAEE France: ANR-11-INBS-0001). We thank Tom Van der Spiet, Anne Cools and the technicians at the University of Barcelona for their help with analyses, Nadine Calluy, Aurélie Dourdain and Joke Van den Berge for their help with logistics and Sara Vicca for her help with statistics.

Figure Legends

Figure 1: Situational map. (A) Detail of north-eastern South America. (B) A detail of northern French Guiana, with its main cities (circles) and the Paracou research station (square). (C) SRTM map of the study site with its 16 permanent plots. (D) Location of the twelve plots used in this study coloured by topographical position (bottom, red; slope, green and top, blue) and also showing the long term undisturbed permanent plot P15 in yellow. (E) Smoothed elevational transect of the studied toposequence with a scaled bottom (red), slope (green) and top (blue) plot depicted. (F) Diagram of the homogenous 20 x 20 m area inside the 50 x 50 m plot wherein the soil core for visual soil classification (star), the bulk density samples (circles) and the samples for chemical, particle size distribution and XRD analysis (triangles) were taken. Adapted from Ferry et al. 2010 and Courtois et al. 2018.

Figure 2: Relationship between clay content (defined as soil particles < 20 μm) and soil C, N and P. Left column are surface soil layer (depth = 0-15 cm) measurements and right column are deeper soil layer (depth = 15-30 cm) measurements. Each dot represents an average of five measurements taken inside the plot. Data gathered in wet and dry season are displayed together.

Figure 3: Relationship between clay content and soil molybdenum, zinc, copper and nickel. Left column are surface soil layer (depth = 0-15 cm) measurements and right column are deeper soil layer (depth = 15-30 cm) measurements. Each dot represents an average of five measurements taken inside the plot. Data gathered in wet and dry season are displayed together. The dashed line represents the limit of detection for the element measured.

Figure 4: Principal component analysis (PCA) of total element concentrations (left) at three topographic positions (middle) and two seasons (right) for two soil depths: 0-15 cm (top) and 15-30 cm (bottom). Elements included in the analysis are C, N, P, K, Mg, Fe, Mo, Cu, Mn, Zn, Ni, V, Cr, As, Sr and Pb. Percentage of variance explained by Principal Component one and two is shown.

Figure 5: Relationship between inorganic P (P_i) measured as Bray P and iron concentration in the soil. Left is surface (0-15 cm depth) soil layer and right is deeper (15-30 cm depth) soil layer. A trend break occurred around 20 g Fe kg^{-1} and higher Fe concentrations were no longer correlated with decreased P_i. Concentrations of Fe are expressed in log_2 scale. Each dot represents an average of five measurements taken inside each plot. Measurements from both seasons are included.

Tables

Table 1 Soil fine fraction physico-chemical properties at the three landscape positions. Values are means, with SE in parentheses, and different superscripted letters indicate statistically significant differences (α = 0.05) between topographic positions. Per topography N = 4 for particle size distribution, N = 8 for mineralogy, N = 20 for bulk density and N = 40 for pH.

Properties	Bottom	Slope	Top
Soil type	Ferric acrisol and gleyic acrisol	Haplic acrisol	Ferralic acrisol and haplic acrisol
Encountered water drainage	Occasional and often presence of water in surface soil	Superficial lateral drainage	Slowed vertical drainage and superficial lateral drainage
Particle size distribution (sand : silt : clay)			
0-15 cm	77:14:9	63:19:18	76:14:10
15–30 cm	75:14:11	59:22:19	71:17:12
Quartz content (%)			
0-15 cm	80.1^{a} (4.4)	64.1^{b} (2.3)	69.3^{b} (4.7)
15–30 cm	74.9^{a} (4.0)	61.0^{b} (3.1)	69.6^{ab} (2.8)
Kaolinite content (%)			
0-15 cm	14.9^{a} (3.0)	26.4^{b} (2.2)	24.5^{b} (3.9)
15–30 cm	18.4^{a} (2.9)	30.1^{b} (3.2)	20.7^{ab} (3.9)
Gibbsite content (%)			
0-15 cm	4.0^{a} (1.5)	4.3^{a} (0.9)	0.4^{b} (0.4)
15–30 cm	4.6^{a} (1.2)	2.7^{a} (0.8)	1.3^{a} (0.6)
Iron (hydr)oxides (%)			
0-15 cm	1.1^{a} (0.1)	5.2^{b} (1.3)	5.8^{b} (2.2)
15–30 cm	2.1^{a} (0.3)	5.8^{a} (1.0)	4.8^{a} (0.6)
Bulk density (g/cm³)			
0-15 cm	1.27^{a} (0.02)	1.07^{a} (0.03)	1.01^{a} (0.03)
15–30 cm	1.40^{a} (0.04)	1.01^{b} (0.06)	1.13^{a} (0.07)
Soil pH			
0-15 cm	4.11^{a} (0.04)	4.02^{ab} (0.03)	3.97^{b} (0.02)
15–30 cm	4.30^{a} (0.01)	4.24^{a} (0.02)	4.26^{a} (0.01)

Table 2 Surface soil (0-15 cm depth) total and available nutrients at the three landscape positions and separated per season. Values are means, with SE in parentheses, and different superscripted letters indicate significant (α = 0.05) differences between topographical positions or seasons according to LMER models. Underlined values were below the machine detection limit (DL S = 1 %, DL Ca = 0.5 % and DL Cd = 0.25 mg kg^{-1})

Season	Wet			Dry		
Topography	Bottom	Slope	Top	Bottom	Slope	Top
Gravimetric Moisture (%)	18.6^{a} (1.9)	23.7^{b} (1.8)	18.5^{a} (2.7)	12.7^{c} (1.3)	17.6^{a} (1.4)	12.6^{c} (1.5)
Volumetric Moisture (%)	23.5^{a} (2.4)	25.5^{a} (4.3)	18.5^{a} (3.9)	16.1^{b} (1.9)	19.1^{b} (3.0)	12.6^{b} (2.1)
Percentage of Field Capacity (%)	123.0^{a} (10.3)	97.3^{a} (7.5)	65.7^{b} (5.6)	67.3^{b} (3.9)	62.7^{b} (6.2)	34.5^{c} (4.5)
C (%)	1.72^{a} (0.12)	2.30^{a} (0.13)	1.86^{a} (0.11)	2.48^{b} (0.12)	2.63^{b} (0.15)	2.13^{b} (0.1)
N (%)	0.13^{a} (0.01)	0.16^{ab} (0.01)	0.14^{ab} (0.01)	0.17^{b} (0.01)	0.18^{b} (0.01)	0.15^{b} (0.01)
P (mg kg^{-1})	80.83^{a} (3.16)	116.74^{b} (6.9)	75.66^{a} (7.87)	88.96^{a} (3.03)	139.38^{b} (6.98)	75.21^{a} (3.3)
C:N	13.27^{a} (0.37)	14.09^{a} (0.21)	13.69^{a} (0.21)	14.43^{b} (0.23)	14.58^{b} (0.4)	14.8^{b} (0.68)
K (mg kg^{-1})	602.22^{a} (93.17)	697.99^{a} (81.70)	562.36^{a} (48.04)	495.53^{a} (23.3)	736.69^{a} (70.73)	613.49^{a} (63.08)
S (mg kg^{-1})	5000 (0)	5000 (0)	5000 (0)	5000 (0)	5000 (0)	5000 (0)
Ca (mg kg^{-1})	300 (0)	300 (0)	300 (0)	300 (0)	300 (0)	300 (0)
Mg (mg kg^{-1})	80.21^{a} (6.64)	86.46^{a} (7.66)	80.04^{a} (7.48)	39.61^{b} (1.63)	42.58^{b} (4.03)	91.07^{a} (3.81)
Fe (mg kg^{-1})	8169^{a} (1660)	26981^{b} (5961)	30433^{b} (5361)	7677^{a} (661)	30391^{b} (2481)	25332^{b} (1491)
Mo (mg kg^{-1})	0.64^{a} (0.11)	0.94^{a} (0.14)	0.94^{a} (0.1)	0.62^{a} (0.18)	1.14^{a} (0.37)	0.43^{a} (0.04)
Cu (mg kg^{-1})	1.75^{a} (0.27)	4.04^{a} (0.48)	2.97^{a} (0.45)	1.92^{a} (0.31)	4.49^{a} (0.26)	2.90^{a} (0.38)

Mn (mg kg^{-1})	20.32^{a} (2.66)	31.79^{ab} (1.05)	41.38^{b} (0.86)	18.06^{a} (0.81)	32.53^{ab} (0.9)	44.17^{b} (3.78)
Na (mg kg^{-1})	79.97^{a} (5.49)	160.26^{a} (6.47)	98.9^{a} (5.38)	77.64^{a} (4.14)	160.42^{a} (12.18)	68.37^{a} (7.13)
Zn (mg kg^{-1})	11.26^{a} (0.9)	21.42^{a} (0.97)	21.71^{a} (1.27)	17.67^{a} (3.72)	26.05^{a} (3.76)	19.00^{a} (1.41)
Ni (mg kg^{-1})	5.00^{a} (0.76)	8.64^{a} (0.4)	7.14^{a} (0.54)	4.95^{a} (1.03)	11.15^{a} (1.62)	6.20^{a} (0.19)
V (mg kg^{-1})	28.59^{a} (3.99)	72.68^{a} (13.45)	80.79^{a} (14.23)	27.4^{a} (1.79)	84.04^{a} (7.57)	61.08^{a} (2.76)
Cr (mg kg^{-1})	30.07^{a} (4.77)	79.07^{a} (15.62)	79.92^{a} (12.01)	19.92^{a} (2.4)	85.97^{a} (10.93)	58.14^{a} (4.5)
As (mg kg^{-1})	0.67^{a} (0.08)	1.67^{a} (0.4)	1.45^{a} (0.26)	0.64^{a} (0.03)	1.86^{a} (0.18)	1.11^{a} (0.08)
Sr (mg kg^{-1})	7.21^{a} (0.33)	8.24^{a} (1.12)	5.92^{a} (0.36)	7.28^{a} (0.53)	7.64^{a} (0.49)	6.54^{a} (0.27)
Pb (mg kg^{-1})	5.20^{a} (0.47)	13.35^{a} (2.57)	4.05^{a} (0.28)	6.20^{a} (0.85)	11.79^{a} (0.44)	3.70^{a} (0.26)
Cd (mg kg^{-1})	0.13 (0)	0.13 (0)	0.13 (0)	0.13 (0)	0.13 (0)	0.13 (0)
NH_4 (mg kg^{-1})	5.20^{a} (0.57)	17.62^{b} (1.62)	11^{ab} (1.49)	2.00^{c} (0.22)	6.68^{d} (0.63)	3.96^{cd} (0.28)
NO_3 (mg kg^{-1})	4.60^{a} (0.37)	7.96^{a} (0.45)	4.30^{a} (0.45)	2.57^{b} (0.13)	4.88^{b} (0.48)	1.90^{b} (0.14)
Olsen P (mg kg^{-1})	2.97^{a} (0.18)	1.71^{b} (0.11)	1.88^{b} (0.15)	2.06^{b} (0.11)	1.26^{c} (0.09)	1.31^{c} (0.07)
Bray P (mg kg^{-1})	3.22^{a} (0.25)	1.29^{bc} (0.09)	1.30^{b} (0.07)	2.76^{d} (0.22)	0.86^{e} (0.07)	1.23^{c} (0.06)

685

Table 3 Deeper soil (15-30 cm depth) total and available nutrients at the three landscape positions and separated per season. Values are means, with SE in parentheses, and different subscripted letters indicate significant (α = 0.05) differences between topographical positions or seasons according to LMER models. Underlined values were below the detection limit (DL S = 1 %, DL Ca = 0.5 % and DL Cd = 0.25 mg kg^{-1})

Season	Wet			Dry		
Topography	Bottom	Slope	Top	Bottom	Slope	Top
Gravimetric Moisture (%)	13.9^{a} (0.9)	20.3^{b} (1.3)	13.2^{a} (1.6)	11.0^{c} (1.2)	16.4^{a} (1.1)	11.0^{c} (1.1)
Volumetric Moisture (%)	19.4^{a} (2.3)	20.2^{a} (3.8)	15.0^{a} (3.3)	15.6^{b} (2.5)	16.5^{b} (3.3)	12.5^{b} (2.4)
Percentage of Field Capacity (%)	81.3^{a} (5.0)	62.5^{ab} (8.6)	47.0^{b} (5.1)	57.0^{b} (4.1)	42.2^{bc} (7.2)	33.9^{c} (4.0)
C (%)	0.84^{ab} (0.08)	1.20^{bc} (0.05)	0.73^{a} (0.03)	1.03^{cd} (0.15)	1.46^{d} (0.07)	0.85^{b} (0.03)
N (%)	0.07^{ab} (0.01)	0.09^{bc} (0.01)	0.06^{a} (0.01)	0.08^{cd} (0.01)	0.11^{d} (0.01)	0.07^{b} (0.01)
P (mg kg^{-1})	68.52^{a} (6.04)	111.55^{b} (4.91)	73.63^{a} (5.81)	83.58^{a} (5.41)	119.17^{b} (4.67)	65.17^{a} (3.51)
C:N	12.03^{a} (0.29)	12.86^{a} (0.24)	12.56^{a} (0.15)	12.45^{a} $(0.33)^{b}$	13.21^{a} $(0.18)^{b}$	12.84^{a} $(0.14)^{b}$
K (mg kg^{-1})	515.87^{a} (32.67)	1015.82^{a} (174.07)	739.98^{a} (86.19)	581.93^{a} (25.06)	781.46^{a} (85.53)	919.74^{a} (214.63)
S (%)	5000 (0)	5000 (0)	5000 (0)	5000 (0)	5000 (0)	5000 (0)
Ca (%)	300 (0)	300 (0)	300 (0)	300 (0)	300 (0)	300 (0)
Mg (mg kg^{-1})	60.82^{a} (8.9)	36.62^{a} (4.36)	46.13^{a} (4.1)	40.07^{a} (5.6)	36.81^{a} (4.92)	46.56^{a} (3.9)
Fe (mg kg^{-1})	10809^{a} (951)	32691^{b} (4495)	41633^{b} (6260)	10357^{a} (1013)	32210^{b} (2899)	34081^{b} (2217)
Mo (mg kg^{-1})	0.7^{a} (0.27)	1.27^{b} (0.36)	0.97^{ab} (0.13)	0.54^{a} (0.13)	1.2^{b} (0.44)	0.67^{ab} (0.07)
Cu (mg kg^{-1})	1.25^{a} (0)	4.35^{b} (0.53)	3.16^{ab} (0.34)	1.51^{a} (0.14)	4.99^{b} (0.37)	3.09^{ab} (0.45)

Mn (mg kg^{-1})	18.85^{a} (0.75)	36.12^{ab} (2.48)	47.21^{b} (3.65)	17.92^{a} (0.58)	31.96^{ab} (1.04)	47.49^{b} (3.13)
Na (mg kg^{-1})	80.12^{a} (6.7)	157.77^{b} (9.77)	104.53^{a} (7.04)	71.4^{a} (3.89)	146.34^{b} (9.6)	88.65^{a} (13.39)
Zn (mg kg^{-1})	10^{a} (0)	25.17^{b} (1.25)	25.88^{b} (1.11)	10^{a} (0)	21.64^{b} (1.42)	28.75^{b} (5.07)
Ni (mg kg^{-1})	5.79^{a} (1.06)	11.5^{b} (1.89)	8.56^{ab} (0.39)	4.97^{a} (0.56)	12.48^{b} (1.87)	8.45^{ab} (0.39)
V (mg kg^{-1})	32.83^{a} (1.69)	95.35^{b} (11.43)	100.44^{b} (13.17)	33.22^{a} (2.03)	94.46^{b} (8.52)	86.26^{b} (5.82)
Cr (mg kg^{-1})	28.1^{a} (2.22)	107.6^{a} (21.8)	87.31^{a} (11.91)	21.86^{a} (1.33)	91.57^{a} (15.15)	72.5^{a} (7.27)
As (mg kg^{-1})	0.71^{a} (0.08)	2.05^{a} (0.23)	2.24^{a} (0.46)	0.8^{a} (0.07)	1.95^{a} (0.16)	1.57^{a} (0.1)
Sr (mg kg^{-1})	7.34^{a} (0.71)	7.00^{a} (0.53)	7.25^{a} (0.69)	7.52^{a} (0.26)	6.93^{a} (0.48)	7.26^{a} (0.38)
Pb (mg kg^{-1})	5.36^{a} (0.7)	12.96^{a} (0.65)	5.19^{a} (0.41)	6.20^{a} (0.25)	13.75^{a} (0.55)	4.78^{a} (0.28)
Cd (mg kg^{-1})	0.13 (0)	0.13 (0)	0.13 (0)	0.13 (0)	0.13 (0)	0.13 (0)
NH_4 (mg kg^{-1})	2.34^{a} (0.24)	7.25^{b} (0.56)	4.07^{a} (0.57)	0.85^{c} (0.11)	3.38^{a} (0.38)	1.47^{c} (0.12)
NO_3 (mg kg^{-1})	3.29^{a} (0.35)	3.07^{a} (0.21)	2.83^{a} (0.38)	1.03^{b} (0.06)	1.77^{b} (0.58)	0.72^{b} (0.14)
OlsenP (mg kg^{-1})	1.08^{a} (0.1)	0.66^{b} (0.1)	0.56^{b} (0.08)	0.95^{a} (0.11)	0.73^{b} (0.05)	0.45^{b} (0.03)
Bray (mg kg^{-1})	1.21^{a} (0.19)	0.34^{b} (0.02)	0.30^{b} (0.02)	1.26^{a} (0.22)	0.38^{b} (0.05)	0.33^{b} (0.03)

692

Supplementary Information

Enzyme extraction:

Extracellular acid phosphatase activity in soil was determined colorimetrically in both seasons in the 0-15 and 15-30 cm soil layers using p-Nitrophenylphosphate substrate, as described in Peguero et al. (2019). Enzyme activity was expressed as µmole of pNP g^{-1} soil DW h^{-1}.

Peguero, G, Sardans, J, Asensio, D, Fernández-Martínez, M, Gargallo-Garriga, A, Grau, O, Llusià, J, Margalef, O, Márquez, L, Ogaya, R, Urbina, I, Courtois, EA, Stahl, C, Van Langenhove, L, Verryckt, LT, Richter, A, Janssens, IA, Peñuelas, J (2019) Nutrient scarcity strengthens soil fauna control over leaf litter decomposition in tropical rainforests. Proceedings of the Royal Society B: Biological Sciences 286 (1910), 20191300. doi:10.1098/rspb.2019.1300

Supplementary Figures

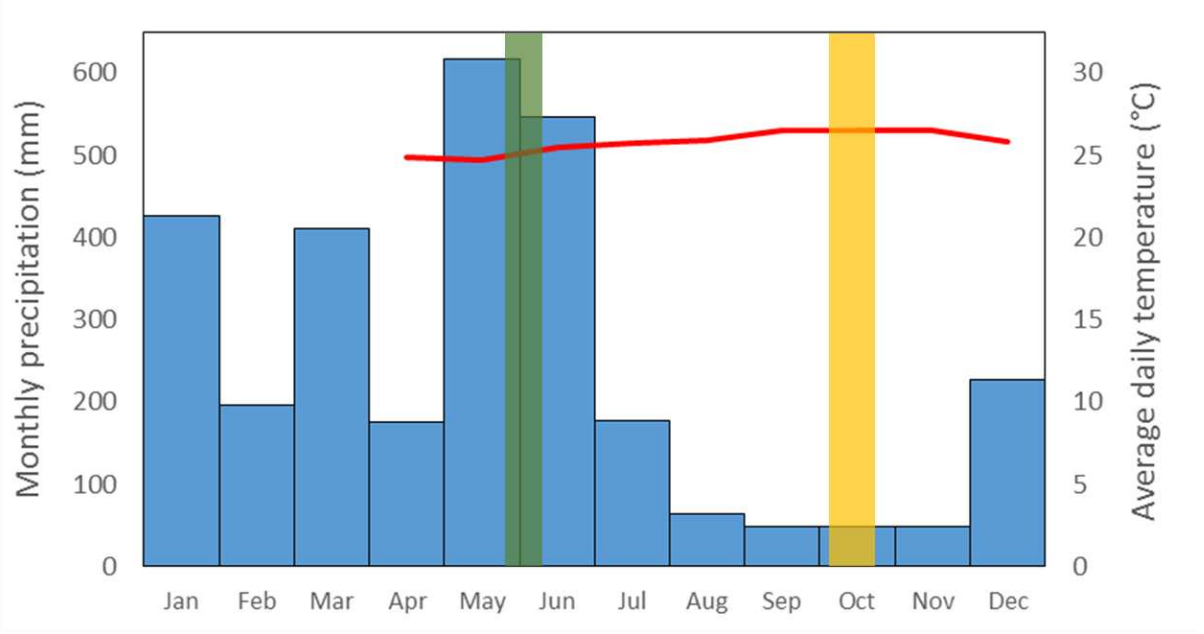

Figure S1 Climate graph for Paracou, 2015. Monthly precipitation (measured with rainfall gauge above the canopy) is shown by blue bars. The red line shows the average daily air temperature. The green bar indicates the wet season sampling period (May 29th – June 10th) and the yellow line indicates the dry season sampling period (October 5th – October 21st). Combined precipitation during the wet season was 2777.4 mm and combined precipitation during the dry season was 209.4 mm. Precipitation and average temperature during the sampling in the wet season was 476 mm and 25.3 °C, respectively. Precipitation and average temperature during the sampling in the dry season was 24 mm and 26.5 °C, respectively.

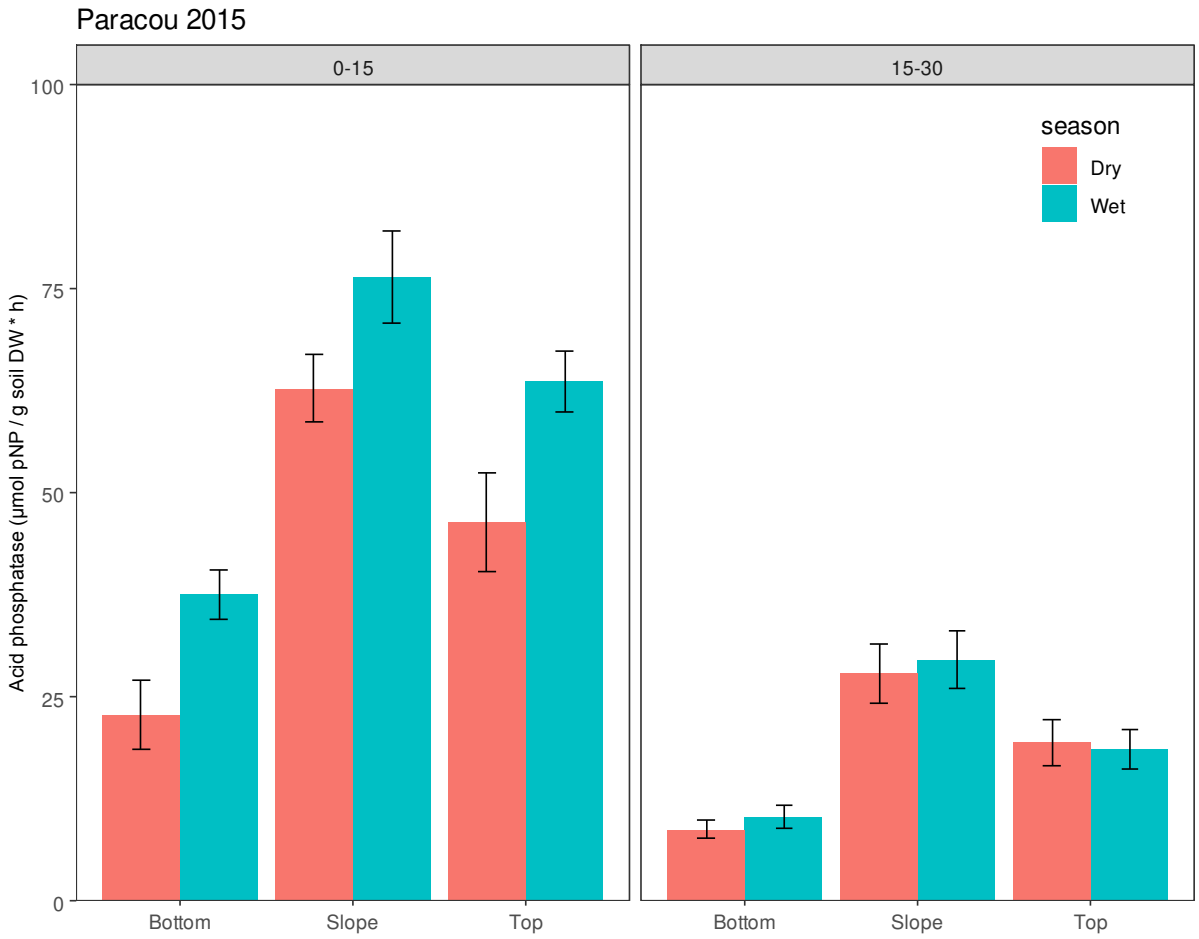

Figure S2 Acid phosphatase (ACP) activity in Paracou soils for a depth of 0-15 cm (left) and 15-30 cm (right). Activity during the dry season (red bars) and wet season (blue bars) is shown for the three sampled topographic units (bottom, slope and top). Error bars represent standard errors and *N* is 20 for each bar. In the upper soil layer (0-15 cm) there is a constant significant (t.test, $P < 0.001$) difference between wet and dry season with higher activities occurring during the wet season. Regarding topographic differences, n both soil depths the ACP activities on the slopes where significantly higher than on the tops, which were in turn significantly higher than on the bottom (lm, $P < 0.001$ for all).

728 Supplementary Tables

729 **Table S1** We used X-ray diffraction (XRD) followed by database matching to
730 identify the common minerals found in the sampled soils. The qualitative
731 mineral phase analysis was performed with the aid of the Powder Diffraction
732 File Data base PDF-4+ 2020 (ICDD, 2016) and through the X'Pert HighScore Plus
733 software, version 4.7, 2017 (Degen et al., 2014). These are the reference
734 numbers used for the identification of each of the different minerals.

735

Mineral	Reference number
Quartz	00-046-1045
Gibbsite	00-033-001
Goethite	01-074-2195
Hematites	00-033-0664
Kaolinite	01-089-6538
	01-078-2109
Nacrite	00-034-0170
	01-076-1781
Lizardite	01-072-1500
Anatase	01-071-1169
Diaspore	01-072-1268
Microcline	01-084-0708
Rutile	01-076-1939

736

Table S2 Linear Pearson correlation coefficients between percentages of clay and silt particles, macro nutrients, micro nutrients and trace metals in soils sampled at two depths. Within depth, no distinction between season was made. Statistically significant correlations ($P < 0.05$) are marked with bold letters. Correlations significant at level $P < 0.01$ are marked with * and correlation significant at level $P < 0.001$ are marked with **. *N* = 10 per plot and per depth (five measures taken in each season)

	Clay	Silt	Pb	Sr	As	Cr	V	Ni	Zn	Mn	Cu	Mo	Fe	Mg	K	P	N
Depth 0-15 cm																	
C	**0.45****	**0.48****	**0.28***	0.12	0.07	0.04	0.02	0.18	**0.31****	0.13	0.13	-0.10	-0.03	0.09	**0.18**	**0.35****	**0.92****
N	**0.49****	**0.51****	**0.38****	0.15	0.01	-0.07	-0.08	0.09	**0.28***	0.06	0.10	-0.11	-0.11	0.02	**0.20**	**0.39****	
P	**0.67****	**0.60****	**0.61****	**0.54****	**0.51****	**0.35****	**0.41****	**0.24***	**0.26***	-0.02	**0.34****	0.10	**0.39****	**-0.21**	**0.19**		
K	**0.28***	**0.31****	0.11	0.10	**0.28***	**0.36****	**0.35****	**0.42****	0.14	**0.38****	**0.43****	0.13	**0.34****	**0.19**			
Mg	-0.04	0.01	-0.04	0.10	0.02	**0.27***	0.15	0.07	0.10	**0.37****	0.14	-0.06	0.16				
Fe	**0.23**	**0.21**	0.05	0.17	**0.90****	**0.91****	**0.98****	**0.43****	**0.35****	**0.47****	**0.70****	**0.34****					
Mo	0.13	0.11	0.05	0.03	**0.35****	**0.39****	**0.35****	**0.79****	0.17	0.11	**0.28***						
Cu	**0.34****	**0.35****	0.16	**0.25***	**0.63****	**0.73****	**0.68****	**0.44****	**0.49****	**0.45****							
Mn	0.17	0.17	-0.02	-0.01	**0.33****	**0.53****	**0.48****	**0.44****	**0.30***								
Zn	**0.33****	**0.39****	**0.22**	0.17	**0.33****	**0.36****	**0.35****	**0.35****									
Ni	**0.35****	**0.36****	0.12	0.05	**0.38****	**0.53****	**0.47****										
V	**0.24***	**0.22**	0.04	0.17	**0.91****	**0.93****											
Cr	**0.22**	**0.22**	0.01	**0.21**	**0.84****												
As	**0.38****	**0.31****	**0.22**	**0.25***													
Sr	**0.30***	**0.18**	**0.64****														
Pb	**0.68****	**0.63****															
Silt	**0.89****																
Depth 15 – 30 cm																	
C	**0.54****	**0.53****	**0.55****	0.04	**0.19**	**0.20**	0.12	**0.25***	0.09	-0.02	**0.33****	**0.20**	0.04	0.03	0.02	**0.59****	**0.97****
N	**0.58****	**0.56****	**0.62****	0.05	0.14	0.12	0.05	**0.25***	0.05	-0.07	**0.23**	**0.20**	-0.05	-0.02	0.01	**0.64****	
P	**0.49****	**0.56****	**0.60****	**0.41****	**0.48****	**0.28***	**0.27***	0.15	0.10	-0.05	**0.36****	**0.20**	**0.23**	-0.13	0.03		

K	**0.24***	**0.22**	0.08	-0.02	**0.19**	**0.38****	**0.36****	**0.19**	**0.21**	**0.25***	**0.31****	0.04	**0.27****	-0.14			
Mg	**-0.23**	**-0.24***	-0.13	0.18	0.15	0.16	0.11	-0.02	0.08	0.05	0.06	0.01	0.09				
Fe	**0.24***	**0.33****	-0.01	0.16	**0.85****	**0.85****	**0.94****	**0.22**	**0.47****	**0.57****	**0.71****	0.17					
Mo	**0.26***	**0.29***	**0.20**	0.10	**0.24***	**0.23**	0.17	**0.82****	0.06	0.12	0.19						
Cu	**0.52****	**0.52****	**0.25***	**0.22**	**0.57****	**0.77****	**0.71****	**0.37****	**0.53****	**0.43****							
Mn	**0.26***	**0.34****	0.03	-0.01	**0.42****	**0.53****	**0.56****	**0.38****	**0.50****								
Zn	**0.25***	**0.39****	0.11	0.14	**0.40****	**0.44****	**0.48****	0.22									
Ni	**0.52****	**0.47****	**0.25***	0.00	0.15	**0.35****	0.26										
V	**0.33****	**0.39****	0.02	0.17	0.86	0.92											
Cr	**0.36****	**0.35****	0.05	0.18	0.74												
As	**0.27***	**0.40****	**0.24**	0.32													
Sr	-0.11	-0.04	0.18														
Pb	**0.65****	**0.66****															
Silt	**0.92****																

742

Table S3 PCA results: Eigenvalues and associated proportion of variance explained by the first 5 principal components (PC)

	PC 1	PC 2	PC 3	PC 4	PC 5
Depth 0 – 15 cm					
Eigenvalues	5.91	2.70	1.72	1.37	1.08
Proportion of Variance explained (%)	36.9	16.9	10.8	8.5	6.7
Cumul explained	36.9	53.8	64.6	73.1	79.8
Depth 15 – 30 cm					
Eigenvalues	5,62	2.97	1.62	1.27	1.03
Proportion of Variance explained (%)	35.1	18.5	10.1	7.9	6.5
Cumul explained	35.1	53.6	63.7	71.6	78.1

Table S4 PCA result: Factor matrix displaying the factor loadings of each variable on components one and two. Loadings > 0.55 are in bold and were considered to correlate well with the corresponding principal component.

	Depth 0 – 15 cm			Depth 15 – 30 cm	
	PC 1	PC 2		PC 1	PC 2
C	0.21	**0.75**		0.40	**0.75**
N	0.14	**0.83**		0.34	**0.82**
P	0.53	**0.58**		0.52	**0.62**
K	0.49	0.06		0.38	0.15
Mg	0.20	0.12		0.10	0.14
Fe	**0.90**	0.27		**0.88**	0.37
Mo	0.46	0.24		0.38	0.24
Cu	**0.81**	0.03		**0.86**	0.04
Mn	**0.56**	0.19		**0.61**	0.35
Zn	0.52	0.25		**0.59**	0.20
Ni	**0.66**	0.07		0.49	0.19
V	**0.91**	0.25		**0.92**	0.31
Cr	**0.91**	0.26		**0.91**	0.23
As	**0.86**	0.09		**0.86**	0.11
Sr	0.33	0.49		0.30	0.11
Pb	0.27	**0.70**		0.34	**0.68**

Table S5 Squared factor loadings for each of the variables at both soil depths. Factor loadings above 0.3 were considered important (bold font).

	0 – 15 cm depth			15 – 30 cm depth	
Variable	PC1	PC2		PC1	PC2
C	0.045	**0.556**		0.150	**0.624**
N	0.020	**0.687**		0.108	**0.743**
P	0.281	**0.357**		0.253	**0.418**

K	0.244	0.004		0.138	0.025
Mg	0.039	0.014		0.009	0.022
Fe	**0.807**	0.072		**0.728**	0.148
Mo	0.214	0.055		0.138	0.066
Cu	**0.650**	0.001		**0.695**	0.001
Mn	**0.317**	0.036		**0.349**	0.135
Zn	0.272	0.060		0.335	0.043
Ni	**0.432**	0.005		0.231	0.041
V	**0.828**	0.063		**0.798**	0.108
Cr	**0.834**	0.066		**0.789**	0.060
As	**0.748**	0.008		**0.704**	0.013
Sr	0.109	0.237		0.083	0.014
Pb	0.070	**0.495**		0.108	**0.508**

752

753 **Table S6** Soil C, N and $\delta^{15}N$ values at the three landscape positions.

	Wet	Wet	Wet	Dry	Dry	Dry
Properties	Bottom	Slope	Top	Bottom	Slope	Top
Soil C (%)	1.72^{a} (0.12)	2.30^{a} (0.13)	1.86^{a} (0.11)	2.48^{b} (0.12)	2.63^{b} (0.15)	2.13^{b} (0.1)
Soil N (%)	0.13^{a} (0.01)	0.16^{a} (0.01)	0.14^{a} (0.01)	0.17^{b} (0.01)	0.18^{b} (0.01)	0.15^{b} (0.01)
$\delta^{15}N$ (‰)	5.56^{a} (0.3)	5.77^{a} (0.26)	4.84^{b} (0.17)	5.84^{a} (0.15)	5.44^{a} (0.13)	4.54^{b} (0.10)
Soil P (mg kg^{-1})	80.83^{a} (3.16)	116.74^{b} (6.9)	75.66^{a} (7.87)	88.96^{c} (3.03)	139.38^{d} (6.98)	75.21^{c} (3.3)
Soil C:N	13.27^{a} (0.37)	14.09^{a} (0.21)	13.69^{a} (0.21)	14.43^{b} (0.23)	14.58^{b} (0.4)	14.8^{b} (0.68)
Soil C:N:P	232 (21) : 17.1 (1.3) : 1	209 (16) : 14.7 (1.0) : 1	278 (21) : 20.4 (1.5) : 1	293 (16) : 20.3 (1.1) : 1	201 (18) : 13.6 (0.8) : 1	302 (18) : 20.3 (0.9) : 1
C stock (kg m^{-2})						
0-15 cm	3.27^{a} (0.22)	3.66^{a} (0.20)	2.76^{b} (0.20)	4.7^{c} (0.25)	4.16^{c} (0.25)	3.25^{a} (0.22)
15-30 cm	1.75^{a} (0.18)	1.75^{a} (0.01)	1.20^{b} (0.06)	2.07^{c} (0.18)	2.13^{c} (0.15)	1.41^{d} (0.08)
N stock (kg m^{-2})						
0-15 cm	0.24^{a} (0.01)	0.26^{a} (0.01)	0.20^{b} (0.01)	0.33^{c} (0.02)	0.29^{c} (0.01)	0.22^{a} (0.01)
15-30 cm	0.14^{a} (0.01)	0.14^{a} (0.01)	0.10^{b} (0.01)	0.16^{c} (0.01)	0.16^{c} (0.01)	0.11^{d} (0.01)
P stock (g m^{-2})						
0-15 cm	15.70^{ab} (0.72)	19.10^{a} (1.31)	11.31^{b} (1.00)	16.82^{ab} (0.71)	21.91^{a} (0.82)	11.21^{b} (0.60)
15-30 cm	14.44^{a} (1.16)	16.43^{a} (0.74)	11.85^{a} (0.80)	17.75^{a} (1.09)	17.85^{a} (0.98)	10.87^{a} (0.86)

754 Notes: Values are means, with SE in parentheses, and different subscripted
755 letters indicate significant ($\alpha = 0.05$) differences between topographical

positions and seasons according to LMER models. Concentrations and $\delta^{15}N$ values are for surface soils, 0-15 cm depth, stocks are taken at two soil depths

References

Aguilos, M, Stahl, C, Burban, B, Hérault, B, Courtois, E, Coste, S, Wagner, F, Ziegler, C, Takagi, K, Bonal, D (2019) Interannual and Seasonal Variations in Ecosystem Transpiration and Water Use Efficiency in a Tropical Rainforest. Forests 10 (1), 14.

Allié, E, Pélissier, R, Engel, J, Petronelli, P, Freycon, V, Deblauwe, V, Soucemarianadin, L, Weigel, J, Baraloto, C (2015) Pervasive Local-Scale Tree-Soil Habitat Association in a Tropical Forest Community. PLoS One 10 (11), e0141488. 10.1371/journal.pone.0141488

Alvarez-Clare, S, Mack, MC, Brooks, M (2013) A direct test of nitrogen and phosphorus limitation to net primary productivity in a lowland tropical wet forest. Ecology 94 (7), 1540-51.

Amundson, R, Jenny, H (1997) On a state factor model of ecosystems. BioScience 47 (8), 536-543. 10.2307/1313122

Anderson, MJ (2017) Permutational Multivariate Analysis of Variance (PERMANOVA). Wiley StatsRef. Stat Ref 15. doi:10.1002/9781118445112.stat07841

Anderson, MJ, Crist, TO, Chase, JM, Vellend, M, Inouye, BD, Freestone, AL, Sanders, NJ, Cornell, HV, Comita, LS, Davies, KF, Harrison, SP, Kraft, NJ, Stegen, JC, Swenson, NG (2011) Navigating the multiple meanings of beta diversity: a roadmap for the practicing ecologist. Ecol Lett 14 (1), 19-28. 10.1111/j.1461-0248.2010.01552.x

Antelo, J, Arce, F, Avena, M, Fiol, S, López, R, Macías, F (2007) Adsorption of a soil humic acid at the surface of goethite and its competitive interaction with phosphate. Geoderma 138 (1), 12-19. https://doi.org/10.1016/j.geoderma.2006.10.011

Barrón, V, Torrent, J (2013) Iron, Manganese and aluminium oxides and oxyhydroxides. In 'Minerals at the Nanoscale'. Eds F Nieto, KJT Livi, O R.) (European Mineralogical Union and the Mineralogical Society of Great Britain & Ireland: London, U. K.)

Bartlett, R, James, B (1980) Studying Dried, Stored Soil Samples — Some Pitfalls1. Soil Science Society of America Journal 44 (4), 721-724. 10.2136/sssaj1980.03615995004400040011x

Birch, HF (1960) Nitrification in soils after different periods of dryness. Plant and Soil 12 (1), 81-96. 10.1007/BF01377763

Birkeland, PW (1999) 'Soils and geomorphology.' (Oxford University Press, New York: New York)

Blancaneaux, P (1973) Notes de pédologie guyanaise. Les Djougoung-Pété du bassin-versant expérimental de la crique Grégoire (Sinnamary - Guyane Française). Cah. ORSTOM, sér. Pédol. XI 14.

Bonan, GB (2008) Forests and Climate Change: Forcings, Feedbacks, and the Climate Benefits of Forests. Science 320 (5882), 1444-1449. 10.1126/science.1155121

Bortoluzzi, EC, Pérez, CAS, Ardisson, JD, Tiecher, T, Caner, L (2015) Occurrence of iron and aluminum sesquioxides and their implications for the P sorption in subtropical soils. Applied Clay Science 104 196-204. https://doi.org/10.1016/j.clay.2014.11.032

Boulet, R (1983) Organisation des couvertures pédologiques des bassins versants ECEREX. Hypothèses sur leur dynamique. Orstom (ed), Le projet ECEREX (Guyane) 30.

Boulet, R, Brugière, JM, Humbel, FX (1979) Relation entre organisation des sols et dynamique de l'eau en Guyane française septentrionale. Conséquences agronomiques d'une évolution déterminée par un déséquilibre d'origine principalement tectonique. Science du Sol (1), 16.

Boulet, R, Lucas, Y, Fritsch, E, Paquet, H Eds H Paquet, N Clauer (1993) 'Géochimie des paysages: le rôle des couvertures pédologiques. In: 'Sédimentologie et Géochimie de la surface' à la memoire de Georges Millot.' (Colloque de l'Academie des Sciences et du Cadas: Paris)

Bray, RH, Kurtz, LT (1945) Determination of Total, Organic, and Available Forms of Phosphorus in Soils. Soil Science 59 (1), 39-46.

Chacón, N, Dezzeo, N, Muñoz, B, Rodríguez, JM (2005) Implications of soil organic carbon and the biogeochemistry of iron and aluminum on soil phosphorus distribution in flooded forests of the lower Orinoco River, Venezuela. Biogeochemistry 73 (3), 555-566. 10.1007/s10533-004-1773-7

Chacón, N, Dezzeo, N, Rangel, M, Flores, S (2008) Seasonal changes in soil phosphorus dynamics and root mass along a flooded tropical forest gradient in the lower Orinoco river, Venezuela. Biogeochemistry 87 (2), 157-168. 10.1007/s10533-007-9174-3

Chacón, N, Flores, S, Gonzalez, A (2006) Implications of iron solubilization on soil phosphorus release in seasonally flooded forests of the lower Orinoco River, Venezuela. Soil Biology and Biochemistry 38 (6), 1494-1499. 10.1016/j.soilbio.2005.10.018

Chadwick, KD, Asner, GP (2016) Tropical soil nutrient distributions determined by biotic and hillslope processes. Biogeochemistry 127 (2), 273-289. 10.1007/s10533-015-0179-z

Chauvel, A, Lucas, Y, Boulet, R (1987) On the genesis of the soil mantle of the region of Manaus, Central Amazonia, Brazil. Experientia 43 (3), 234-241. 10.1007/bf01945546

Chave, J, Navarrete, D, Almeida, S, Álvarez, E, Aragão, LEOC, Bonal, D, Châtelet, P, Silva-Espejo, JE, Goret, JY, von Hildebrand, P, Jiménez, E, Patiño, S, Peñuela, MC, Phillips, OL, Stevenson, P, Malhi, Y (2010) Regional and seasonal patterns of litterfall in tropical South America. Biogeosciences 7 (1), 43-55. 10.5194/bg-7-43-2010

Chaves, J, Neill, C, Germer, S, Gouveia Neto, S, Krusche, AV, Castellanos Bonilla, A, Elsenbeer, H (2009) Nitrogen Transformations in Flowpaths Leading from Soils to Streams in Amazon Forest and Pasture. Ecosystems 12 (6), 961-972. 10.1007/s10021-009-9270-4

Clark, DA (2004) Tropical Forests and Global Warming: Slowing It down or Speeding It up? Frontiers in Ecology and the Environment 2 (2), 73-80. 10.2307/3868213

Cleveland, CC, Townsend, AR, Constance, BC, Ley, RE, Schmidt, SK (2004) Soil Microbial Dynamics in Costa Rica: Seasonal and Biogeochemical Constraints. Biotropica 36 (2), 184-195. 10.1111/j.1744-7429.2004.tb00311.x

Cleveland, CC, Townsend, AR, Taylor, P, Alvarez-Clare, S, Bustamante, MMC, Chuyong, G, Dobrowski, SZ, Grierson, P, Harms, KE, Houlton, BZ, Marklein, A, Parton, W, Porder, S, Reed, SC, Sierra, CA, Silver, WL, Tanner, EVJ, Wieder, WR (2011) Relationships among net primary productivity, nutrients and climate in tropical rain forest: a pan-tropical analysis. Ecol Lett 14 (9), 939-947. doi:10.1111/j.1461-0248.2011.01658.x

Courtois, EA, Stahl, C, Van den Berge, J, Bréchet, L, Van Langenhove, L, Richter, A, Urbina, I, Soong, JL, Peñuelas, J, Janssens, IA (2018) Spatial Variation of Soil CO2, CH4 and N2O Fluxes Across Topographical Positions in Tropical Forests of the Guiana Shield. Ecosystems 10.1007/s10021-018-0232-6

Crews, TE, Kitayama, K, Fownes, JH, Riley, RH, Herbert, DA, Mueller-Dombois, D, Vitousek, PM (1995) Changes in Soil Phosphorus Fractions and Ecosystem Dynamics across a Long Chronosequence in Hawaii. Ecology 76 (5), 1407-1424. 10.2307/1938144

Cuevas, E, Medina, E (1986) Nutrient dynamics within amazonian forest ecosystems. Oecologia 68 (3), 466-472. 10.1007/bf01036756

Degen, T, Sadki, M, Bron, E, König, U, Nénert, G (2014) The HighScore suite. Powder Diffraction 29 (S2), S13-S18. 10.1017/S0885715614000840

Do Nascimento, NR, Bueno, GT, Fritsch, E, Herbillon, AJ, Allard, T, Melfi, AJ, Astolfo, R, Boucher, H, Li, Y (2004) Podzolization as a deferralitization process: a study of an Acrisol–Podzol sequence derived from Palaeozoic sandstones in the northern upper Amazon Basin. European Journal of Soil Science 55 (3), 523-538. doi:10.1111/j.1365-2389.2004.00616.x

Dray, S, Dufour, AB (2007) The ade4 package: implementing the duality diagram for ecologists. Journal of Statistical Software 22 (4), 21.

Driessen, P, Deckers, J, Spaargaren, O, Nachtergaele, F (2001) Lecture notes on the major soils of the world. FAO, Rome. Available

Dubroeucq, D, Volkoff, B (1998) From Oxisols to Spodosols and Histosols: evolution of the soil mantles in the Rio Negro basin (Amazonia). Catena 32 (3), 245-280. https://doi.org/10.1016/S0341-8162(98)00045-9

Epron, D, Bosc, A, Bonal, D, Freycon, V (2006) Spatial variation of soil respiration across a topographic gradient in a tropical rain forest in French Guiana. Journal of Tropical Ecology 22 (5), 565-574. 10.1017/S0266467406003415

FAO (1998) World Reference Base for Soil Resources. Rome. Available

Ferry, B, Morneau, F, Bontemps, J-D, Blanc, L, Freycon, V (2010) Higher treefall rates on slopes and waterlogged soils result in lower stand biomass and productivity in a tropical rain forest. Journal of Ecology 98 (1), 106-116. 10.1111/j.1365-2745.2009.01604.x

Fierer, N, Schimel, JP, Holden, PA (2003) Influence of Drying–Rewetting Frequency on Soil Bacterial Community Structure. Microbial Ecology 45 (1), 63-71. 10.1007/s00248-002-1007-2

Fink, JR, Inda, AV, Tiecher, T, Barrón, V (2016) Iron oxides and organic matter on soil phosphorus availability. Ciência e Agrotecnologia 40 369-379.

Fritsch, E, Bocquier, G, Boulet, R, Dosso, M, Humbel, FX (1986) Les systèmes transformants d'une couverture ferralitique de Guyane française: Analyse structurale d'une formation supergène et mode de représentation. Cah. ORSTOM, sér. Pédol. 22 (4), 35.

Fritsch, E, Fitzpatrick, R (1994) Interpretation of soil features produced by ancient and modern processes in degraded landscapes .1. A new method for constructing conceptual soil-water-landscape models. Soil Research 32 (5), 889-907. https://doi.org/10.1071/SR9940889

Gee, GW, Bauder, JW (1986) Particle-size analysis. In ' Methods of Soil Analysis Part 1: Physical and Mineralogical Methods'. (Ed. A Kute.) p. 29. (American Society of Agronomy & Soil Science Society of America: Madison, Wisconsin, USA)

González-Costa, JJ, Reigosa, MJ, Matías, JM, Fernández-Covelo, E (2017) Analysis of the Importance of Oxides and Clays in Cd, Cr, Cu, Ni, Pb and Zn Adsorption and Retention with Regression Trees. PLoS One 12 (1), e0168523-e0168523. 10.1371/journal.pone.0168523

Gourlet-Fleury, S, Guehl, JM, Laroussinie, O (2004) 'Ecology and management of a neotropical rainforest. Lessons drawn from Paracou, a long-term experimental research site in French Guiana.' (Elsevier: Meppel, The Netherlands)

Gransee, A, Führs, H (2012) Magnesium mobility in soils as a challenge for soil and plant analysis, magnesium fertilization and root uptake under adverse growth conditions. Plant and Soil 368 (1-2), 5-21. 10.1007/s11104-012-1567-y

Grau, O, Penuelas, J, Ferry, B, Freycon, V, Blanc, L, Desprez, M, Baraloto, C, Chave, J, Descroix, L, Dourdain, A, Guitet, S, Janssens, IA, Sardans, J, Herault, B (2017) Nutrient-cycling mechanisms other than the direct absorption from soil may control forest structure and dynamics in poor Amazonian soils. Sci Rep 7 45017. 10.1038/srep45017

Gross, A, Pett-Ridge, J, Silver, W (2018) Soil Oxygen Limits Microbial Phosphorus Utilization in Humid Tropical Forest Soils. Soil Systems 2 (4), 65.

Guehl, J, M. (1984) Dynamique de l'eau dans le sol en forêt tropicale humide guyanaise. Influence de la couverture pédologique. Ann. For. Sci. 41 (2), 195-236.

Guitet, S, Freycon, V, Brunaux, O, Pélissier, R, Sabatier, D, Couteron, P (2015) Geomorphic control of rain-forest floristic composition in French Guiana: more than a soil filtering effect? Journal of Tropical Ecology 32 (1), 22-40. 10.1017/s0266467415000620

Gustafsson, JP, Pechová, P, Berggren, D (2003) Modeling Metal Binding to Soils: The Role of Natural Organic Matter. Environmental Science & Technology 37 (12), 2767-2774. 10.1021/es026249t

Hall, SJ, Silver, WL (2015) Reducing conditions, reactive metals, and their interactions can explain spatial patterns of surface soil carbon in a humid tropical forest. Biogeochemistry 125 (2), 149-165. 10.1007/s10533-015-0120-5

Hammond, D (2005) 'Tropical Forests of the Guiana Shield: Ancient Forests in a Modern World.' (CABI Publishing: Cambridge)

Harter, RD, Naidu, R (1995) Role of Metal-Organic complexation in metal sorption by Soils. In 'Advances in Agronomy'. (Ed. DL Sparks.) Vol. 55, pp. 219-263. (Academic Press:

Heimsath, AM, Dietrich, WE, Nishiizumi, K, Finkel, RC (1997) The soil production function and landscape equilibrium. Nature 388 358. 10.1038/41056

Helfenstein, J, Jegminat, J, McLaren, TI, Frossard, E (2018) Soil solution phosphorus turnover: derivation, interpretation, and insights from a global compilation of isotope exchange kinetic studies. Biogeosciences 15 (1), 105-114. 10.5194/bg-15-105-2018

Henrot, J, Robertson, GP (1994) Vegetation removal in two soils of the humid tropics: Effect on microbial biomass. Soil Biology and Biochemistry 26 (1), 111-116. https://doi.org/10.1016/0038-0717(94)90202-X

Hernández-Soriano, MC (2012) The Role of Aluminum-Organo Complexes in Soil Organic Matter Dynamics. In 'Soil Health and Land Use Management'. (Ed. MC Hernández-Soriano.) (IntechOpen: Leuven, BE)

Horbe, AMC, Horbe, MA, Suguio, K (2004) Tropical Spodosols in northeastern Amazonas State, Brazil. Geoderma 119 (1), 55-68. https://doi.org/10.1016/S0016-7061(03)00233-7

Jenny, H (1941) 'Factors of soil formation: a system of quantitative pedology.' (McGraw-Hill, New York: New York)

Jobbágy, EG, Jackson, RB (2000) The Vertical Distribution of Soil Organic Carbon and Its Relation to Climate and Vegetation. Ecological Applications 10 (2), 423-436. 10.2307/2641104

Kaspari, M, Garcia, MN, Harms, KE, Santana, M, Wright, SJ, Yavitt, JB (2008) Multiple nutrients limit litterfall and decomposition in a tropical forest. Ecol Lett 11 (1), 35-43. 10.1111/j.1461-0248.2007.01124.x

Koehler, B, Corre, MD, Veldkamp, E, Wullaert, H, Wright, SJ (2009) Immediate and long-term nitrogen oxide emissions from tropical forest soils exposed to elevated nitrogen input. Global Change Biology 15 (8), 2049-2066. 10.1111/j.1365-2486.2008.01826.x

Kroonenberg, SB, de Roever, EWF, Fraga, LM, Reis, NJ, Faraco, T, Lafon, JM, Cordani, U, Wong, TE (2016) Paleoproterozoic evolution of the Guiana Shield in Suriname: A revised model. Netherlands Journal of Geosciences - Geologie en Mijnbouw 95 (4), 491-522. 10.1017/njg.2016.10

Kuznetsova, A, Brockhoff, PB, Christensen, RHB (2017) lmerTest Package: Tests in Linear Mixed Effects Models. Journal of Statistical Software 82 (13), 27.

924 Labrière, N, Locatelli, B, Laumonier, Y, Freycon, V, Bernoux, M (2015) Soil erosion in the humid tropics: A
925 systematic quantitative review. Agriculture, Ecosystems & Environment 203 127-139.
926 https://doi.org/10.1016/j.agee.2015.01.027

927 Lagaly, G, Barrer, RM, Goulding, K (1984) Clay-Organic Interactions [and Discussion]. Philosophical
928 Transactions of the Royal Society of London. Series A, Mathematical and Physical Sciences 311 (1517), 315-332.

929 Larsen, MC, Torres-Sánchez, AJ, Concepción, IM (1999) Slopewash, surface runoff and fine-litter transport in
930 forest and landslide scars in humid-tropical steeplands, luquillo experimental forest, Puerto Rico. Earth Surface
931 Processes and Landforms 24 (6), 481-502. doi:10.1002/(SICI)1096-9837(199906)24:6<481::AID-
932 ESP967>3.0.CO;2-G

933 Laurance, WF, Fearnside, PM, Laurance, SG, Delamonica, P, Lovejoy, TE, Rankin-de Merona, JM, Chambers,
934 JQ, Gascon, C (1999) Relationship between soils and Amazon forest biomass: a landscape-scale study. Forest
935 Ecology and Management 118 (1), 127-138. https://doi.org/10.1016/S0378-1127(98)00494-0

936 Lee, YB, Lorenz, N, Dick, LK, Dick, RP (2007) Cold Storage and Pretreatment Incubation Effects on Soil
937 Microbial Properties. Soil Science Society of America Journal 71 (4), 1299-1305. 10.2136/sssaj2006.0245

938 Lodge, DJ, McDowell, WH, McSwiney, CP (1994) The importance of nutrient pulses in tropical forests.
939 Trends in Ecology & Evolution 9 (10), 384-387. https://doi.org/10.1016/0169-5347(94)90060-4

940 Lucas, Y, Chauvel, A (1992) Soil formation in tropically weathered terrains. In: Butt CRM and Zeegers H
941 (Eds) Handbook of exploration geochemistry. Soil, laterite and saprolite geochemistry in mineral exploration of
942 tropically weathered terrains (pp 57-76). Elsevier)

943 Lucas, Y, Nahon, BD, Cornu, S, Eyrolle, F (1996) Genèse et fonctionnement des sols en milieu équatorial.
944 Comptes Rendus de l'Académie des Sciences Série IIa, Paris 322 1-16.

945 Luizao, RCC, Bonde, TA, Rosswall, T (1992) Seasonal variation of soil microbial biomass—The effects of
946 clearfelling a tropical rainforest and establishment of pasture in the central Amazon. Soil Biology and
947 Biochemistry 24 (8), 805-813. https://doi.org/10.1016/0038-0717(92)90256-W

948 Luizão, RCC, Luizão, FJ, Paiva, RQ, Monteiro, TF, Sousa, LS, Kruijt, B (2004) Variation of carbon and nitrogen
949 cycling processes along a topographic gradient in a central Amazonian forest. Global Change Biology 10 (5),
950 592-600. doi:10.1111/j.1529-8817.2003.00757.x

951 Margalef, O, Sardans, J, Fernández-Martínez, M, Molowny-Horas, R, Janssens, IA, Ciais, P, Goll, D, Richter, A,
952 Obersteiner, M, Asensio, D, Peñuelas, J (2017) Global patterns of phosphatase activity in natural soils. Scientific
953 Reports 7 (1), 1337. 10.1038/s41598-017-01418-8

954 McGrath, DA, Comerford, NB, Duryea, ML (2000) Litter dynamics and monthly fluctuations in soil
955 phosphorus availability in an Amazonian agroforest. Forest Ecology and Management 131 (1), 167-181.
956 https://doi.org/10.1016/S0378-1127(99)00207-8

957 McGroddy, ME, Silver, WL (2011) Biogeochemical cycling in tropical forests. In 'Tropical Rainforest
958 Responses to Climatic Change'. Eds M Bush, J Flenley, W Gosling.) pp. 315-341. (Springer Berlin Heidelberg:
959 Berlin, Heidelberg)

960 McSwiney, CP, MCDowell, WH, Keller, M (2001) Distribution of nitrous oxide and regulators of its
961 production across a tropical rainforest catena in the Luquillo Experimental Forest, Puerto Rico. Biogeochemistry
962 56 22.

963 Mesić, M, Kisić, I, Bašić, F, Butorac, A, Zgorelec, Ž, Gašpar, I (2007) Losses of Ca, Mg and SO4 2-S with
964 drainage water at fertilisation with different nitrogen rates. Agriculturae Conspectus Scientificus 72 (1), 53-58.

965 Myneni, RB, Yang, W, Nemani, RR, Huete, AR, Dickinson, RE, Knyazikhin, Y, Didan, K, Fu, R, Negrón Juárez,
966 RI, Saatchi, SS, Hashimoto, H, Ichii, K, Shabanov, NV, Tan, B, Ratana, P, Privette, JL, Morisette, JT, Vermote, EF,
967 Roy, DP, Wolfe, RE, Friedl, MA, Running, SW, Votava, P, El-Saleous, N, Devadiga, S, Su, Y, Salomonson, VV

(2007) Large seasonal swings in leaf area of Amazon rainforests. Proceedings of the National Academy of Sciences 104 (12), 4820. 10.1073/pnas.0611338104

Nahon, BD (1991) 'Introduction to the petrology of soils and chemical weathering.' (John Wiley & Sons, Inc.:

Nardoto, GB, Ometto, JPHB, Ehleringer, JR, Higuchi, N, Bustamante, MMdC, Martinelli, LA (2008) Understanding the Influences of Spatial Patterns on N Availability Within the Brazilian Amazon Forest. Ecosystems 11 (8), 1234-1246. 10.1007/s10021-008-9189-1

Nemani, RR, Keeling, CD, Hashimoto, H, Jolly, WM, Piper, SC, Tucker, CJ, Myneni, RB, Running, SW (2003) Climate-Driven Increases in Global Terrestrial Net Primary Production from 1982 to 1999. Science 300 (5625), 1560-1563. 10.1126/science.1082750

Oksanen, J, Guillaume, B, Friendly, M, Kindt, R, Legendre, P, McGlinn, D, Minchin, PR, O'Hara, RB, Simpson, GL, Solymos, P, Stevens, HH, Szoecs, E, Wagner, H (2019) 'vegan: Community Ecology Package.'

Olsen, SR, Cole, CV, Watanabe, FS (1954) 'Estimation of available phosphorus in soils by extraction with sodium bicarbonate.' (USDA: Washington)

Osborne, BB, Nasto, MK, Asner, GP, Balzotti, CS, Cleveland, CC, Sullivan, BW, Taylor, PG, Townsend, AR, Porder, S (2017) Climate, Topography, and Canopy Chemistry Exert Hierarchical Control Over Soil N Cycling in a Neotropical Lowland Forest. Ecosystems 20 (6), 1089-1103. 10.1007/s10021-016-0095-7

Pierzynski, GM, McDowell, R (2005) Chemistry, Cycling, and Potential Movement of Inorganic Phosphorus in Soils. In 'Phosphorus: Agriculture and the Environment'. pp. 53-86. Madiosn, WI)

Porder, S, Asner, GP, Vitousek, PM (2005) Ground-based and remotely sensed nutrient availability across a tropical landscape. Proc Natl Acad Sci U S A 102 (31), 10909-10912. 10.1073/pnas.0504929102

Quenea, K, Lamy, I, Winterton, P, Bermond, A, Dumat, C (2009) Interactions between metals and soil organic matter in various particle size fractions of soil contaminated with waste water. Geoderma 149 (3), 217-223. https://doi.org/10.1016/j.geoderma.2008.11.037

Quesada, CA, Lloyd, J, Anderson, LO, Fyllas, NM, Schwarz, M, Czimczik, CI (2011) Soils of Amazonia with particular reference to the RAINFOR sites. Biogeosciences 8 (6), 1415-1440. 10.5194/bg-8-1415-2011

Quesada, CA, Lloyd, J, Schwarz, M, Patiño, S, Baker, TR, Czimczik, C, Fyllas, NM, Martinelli, L, Nardoto, GB, Schmerler, J, Santos, AJB, Hodnett, MG, Herrera, R, Luizão, FJ, Arneth, A, Lloyd, G, Dezzeo, N, Hilke, I, Kuhlmann, I, Raessler, M, Brand, WA, Geilmann, H, Moraes Filho, JO, Carvalho, FP, Araujo Filho, RN, Chaves, JE, Cruz Junior, OF, Pimentel, TP, Paiva, R (2010) Variations in chemical and physical properties of Amazon forest soils in relation to their genesis. Biogeosciences 7 (5), 1515-1541. 10.5194/bg-7-1515-2010

R Core Team (2018) R: A Language and Environment for Statistical Computing. R Foundation for Statistical Computing 3.5

Randerson, JT, Hoffman, FM, Thornton, PE, Mahowald, NM, Lindsay, K, Lee, Y-H, Nevison, CD, Doney, SC, Bonan, G, Stöckli, R, Covey, C, Running, SW, Fung, IY (2009) Systematic assessment of terrestrial biogeochemistry in coupled climate–carbon models. Global Change Biology 15 (10), 2462-2484. doi:10.1111/j.1365-2486.2009.01912.x

Renard, KG, Foster, GR, Weesies, GA, McCool, D, Yoder, D (1997) 'Predicting soil erosion by water: a guide to conservation planning with the revised universal soil loss equation (RUSLE).' (U.S. Department of Agriculture: Washington DC)

Roering, JJ, Kirchner, JW, Dietrich, WE (1999) Evidence for nonlinear, diffusive sediment transport on hillslopes and implications for landscape morphology. Water Resources Research 35 (3), 853-870. doi:10.1029/1998WR900090

Sabatier, D, Grimaldi, M, Prévost, M-F, Guillaume, J, Godron, M, Dosso, M, Curmi, P (1997) The influence of soil cover organization on the floristic and structural heterogeneity of a Guianan rain forest. Plant Ecology 131 (1), 81-108. 10.1023/a:1009775025850

Sanchez, PA (1977) Properties and Management of Soils in the Tropics. Soil Science 124 (3), 187.

Sarkar, JM, Leonowicz, A, Bollag, J-M (1989) Immobilization of enzymes on clays and soils. Soil Biology and Biochemistry 21 (2), 223-230. https://doi.org/10.1016/0038-0717(89)90098-9

Scatena, FN, Lugo, AE (1995) Geomorphology, disturbance, and the soil and vegetation of two subtropical wet steepland watersheds of Puerto Rico. Geomorphology 13 15.

Schaap, MG, Leij, FJ, van Genuchten, MT (2001) rosetta: a computer program for estimating soil hydraulic parameters with hierarchical pedotransfer functions. Journal of Hydrology 251 (3), 163-176. https://doi.org/10.1016/S0022-1694(01)00466-8

Setter, TL, Waters, I (2003) Review of prospects for germplasm improvement for waterlogging tolerance in wheat, barley and oats. Plant and Soil 253 (1), 1-34. 10.1023/A:1024573305997

Sibanda, HM, Young, SD (1986) Competitive adsorption of humus acids and phosphate on goethite, gibbsite and two tropical soils. Journal of Soil Science 37 (2), 197-204. doi:10.1111/j.1365-2389.1986.tb00020.x

Singh, JS, Raghubanshi, AS, Singh, RS, Srivastava, SC (1989) Microbial biomass acts as a source of plant nutrients in dry tropical forest and savanna. Nature 338 (6215), 499-500. 10.1038/338499a0

Singh, RS, Srivastava, SC, Raghubanshi, AS, Singh, JS, Singh, SP (1991) Microbial C, N and P in Dry Tropical Savanna: Effects of Burning and Grazing. Journal of Applied Ecology 28 (3), 869-878. 10.2307/2404213

Sinsabaugh, RL, Shah, JJF (2012) Ecoenzymatic Stoichiometry and Ecological Theory. Annual Review of Ecology, Evolution, and Systematics 43 (1), 313-343. 10.1146/annurev-ecolsys-071112-124414

Smeck, NE (1973) 'Phosphorus: An Indicator of Pedogenetic Weathering Processes.'

Smith, AP, Marín-Spiotta, E, Balser, T (2015) Successional and seasonal variations in soil and litter microbial community structure and function during tropical postagricultural forest regeneration: a multiyear study. Glob Chang Biol 21 (9), 3532-47. 10.1111/gcb.12947

Sollins, P (1998) FACTORS INFLUENCING SPECIES COMPOSITION IN TROPICAL LOWLAND RAIN FOREST: DOES SOIL MATTER? Ecology 79 (1), 23-30. 10.1890/0012-9658(1998)079[0023:fiscit]2.0.co;2

Soong, JL, Janssens, IA, Grau, O, Margalef, O, Stahl, C, Van Langenhove, L, Urbina, I, Chave, J, Dourdain, A, Ferry, B, Freycon, V, Herault, B, Sardans, J, Penuelas, J, Verbruggen, E (2020) Soil properties explain tree growth and mortality, but not biomass, across phosphorus-depleted tropical forests. Sci Rep 10 (1), 2302. 10.1038/s41598-020-58913-8

Sparling, G, Whale, K, Ramsay, A (1985) Quantifying the contribution from the soil microbail biomass to the extractable P levels of fresh and air-dried soils. Soil Research 23 (4), 613-621. https://doi.org/10.1071/SR9850613

Sposito, G (1996) 'The Environmental Chemistry of Aluminum.' (Lewis Publishers: Boca Raton, FL)

Srivastava, SC (1992) Microbial c, n and p in dry tropical soils: Seasonal changes and influence of soil moisture. Soil Biology and Biochemistry 24 (7), 711-714. https://doi.org/10.1016/0038-0717(92)90050-8

Tack, FMG, Van Ranst, E, Lievens, C, Vandenberghe, RE (2006) Soil solution Cd, Cu and Zn concentrations as affected by short-time drying or wetting: The role of hydrous oxides of Fe and Mn. Geoderma 137 (1), 83-89. https://doi.org/10.1016/j.geoderma.2006.07.003

Tiessen, H, Chacon, P, Cuevas, E (1994) Phosphorus and nitrogen status in soils and vegetation along a toposequence of dystrophic rainforests on the upper Rio Negro. Oecologia 99 (1), 145-150. 10.1007/bf00317095

Tiessen, H, Stewart, JWB, Cole, CV (1984) Pathways of Phosphorus Transformations in Soils of Differing Pedogenesis1. Soil Science Society of America Journal 48 (4), 853-858. 10.2136/sssaj1984.03615995004800040031x

Townsend, AR, Asner, GP, Cleveland, CC (2008) The biogeochemical heterogeneity of tropical forests. Trends in Ecology & Evolution 23 (8), 424-431. https://doi.org/10.1016/j.tree.2008.04.009

Townsend, AR, Cleveland, CC, Houlton, BZ, Alden, CB, White, JW (2011) Multi-element regulation of the tropical forest carbon cycle. Frontiers in Ecology and the Environment 9 (1), 9-17. doi:10.1890/100047

Turner, BL, Haygarth, PM (2001) Phosphorus solubilization in rewetted soils. Nature 411 258. 10.1038/35077146

Turner, BL, Yavitt, JB, Harms, KE, Garcia, MN, Romero, TE, Wright, SJ (2013) Seasonal Changes and Treatment Effects on Soil Inorganic Nutrients Following a Decade of Fertilizer Addition in a Lowland Tropical Forest. Soil Science Society of America Journal 77 (4), 1357-1369. 10.2136/sssaj2012.0128

Turner, BL, Yavitt, JB, Harms, KE, Garcia, MN, Wright, SJ (2015) Seasonal changes in soil organic matter after a decade of nutrient addition in a lowland tropical forest. Biogeochemistry 123 (1-2), 221-235. 10.1007/s10533-014-0064-1

Van Genuchten, MT (1980) A Closed-Form Equation for Predicting the Hydraulic Conductivity of Unsaturated Soils. Soil Science Society of America Journal 44 (5), 892.

Vitousek, P, Chadwick, O, Matson, P, Allison, S, Derry, L, Kettley, L, Luers, A, Mecking, E, Monastra, V, Porder, S (2003) Erosion and the Rejuvenation of Weathering-derived Nutrient Supply in an Old Tropical Landscape. Ecosystems 6 (8), 762-772. 10.1007/s10021-003-0199-8

Vitousek, PM, Howarth, RW (1991) Nitrogen limitation on land and in the sea: How can it occur? Biogeochemistry 13 (2), 87-115. 10.1007/bf00002772

Vitousek, PM, Sanford, RL (1986) Nutrient Cycling in Moist Tropical Forest. Annual Review of Ecology and Systematics 17 137-167. DOI 10.1146/annurev.es.17.110186.001033

Wagner, F, Rossi, V, Stahl, C, Bonal, D, Hérault, B (2013) Asynchronism in leaf and wood production in tropical forests: a study combining satellite and ground-based measurements. Biogeosciences 10 (11), 7307-7321. 10.5194/bg-10-7307-2013

Walker, TW (1964) 'The significance of phosphorus in pedogenesis.' Butterworths, London)

Walker, TW, Syers, JK (1976) The fate of phosphorus during pedogenesis. Geoderma 15 (1), 1-19. https://doi.org/10.1016/0016-7061(76)90066-5

Weintraub, SR, Taylor, PG, Porder, S, Cleveland, CC, Asner, GP, Townsend, AR (2015) Topographic controls on soil nitrogen availability in a lowland tropical forest. Ecology 96 (6), 1561-1574. doi:10.1890/14-0834.1

Wickham, H (2016) 'ggplot2: Elegant graphics for Data Analysis.' (Springer-Verlag: New York)

Wickham, H, François, R, Henry, L, Müller, K (2018) 'dplyr: A Grammar of Data Manipulation.'

Wieder, RK, Wright, SJ (1995) Tropical Forest Litter Dynamics and Dry Season Irrigation on Barro Colorado Island, Panama. Ecology 76 (6), 1971-1979. 10.2307/1940727

Wright, SJ, Yavitt, JB, Wurzburger, N, Turner, BL, Tanner, EVJ, Sayer, EJ, Santiago, LS, Kaspari, M, Hedin, LO, Harms, KE, Garcia, MN, Corre, MD (2011) Potassium, phosphorus, or nitrogen limit root allocation, tree growth, or litter production in a lowland tropical forest. Ecology 92 (8), 1616-1625. 10.1890/10-1558.1

1092 Yamashita, N, Ohta, S, Sase, H, Luangjame, J, Visaratana, T, Kievuttinon, B, Garivait, H, Kanzaki, M (2010)
1093 Seasonal and spatial variation of nitrogen dynamics in the litter and surface soil layers on a tropical dry
1094 evergreen forest slope. Forest Ecology and Management 259 (8), 1502-1512.
1095 https://doi.org/10.1016/j.foreco.2010.01.026

1096 Yan, J, Jiang, T, Yao, Y, Lu, S, Wang, Q, Wei, S (2016) Preliminary investigation of phosphorus adsorption
1097 onto two types of iron oxide-organic matter complexes. Journal of Environmental Sciences 42 152-162.
1098 https://doi.org/10.1016/j.jes.2015.08.008

1099 Yang, X, Post, WM, Thornton, PE, Jain, A (2013) The distribution of soil phosphorus for global
1100 biogeochemical modeling. Biogeosciences 10 (4), 2525-2537. 10.5194/bg-10-2525-2013

1101 Yavitt, JB, Wright, SJ (1996) Temporal patterns of soil nutrients in a Panamanian moist forest revealed by
1102 ion-exchange resin and experimental irrigation. Plant and Soil 183 (1), 117-129. 10.1007/BF02185571

1103 Yokobe, T, Hyodo, F, Tokuchi, N (2018) Seasonal Effects on Microbial Community Structure and Nitrogen
1104 Dynamics in Temperate Forest Soil. Forests 9 (3), 153. 10.3390/f9030153

1105 Zinn, YL, Lal, R, Resck, DVS (2005) Texture and organic carbon relations described by a profile pedotransfer
1106 function for Brazilian Cerrado soils. Geoderma 127 (1), 168-173.
1107 https://doi.org/10.1016/j.geoderma.2005.02.010

1108